

**STUDIES ON THE MECHANISM OF PHOTODAMAGE AND
PHOTOPROTECTION OF PHOTOSYSTEM II IN THE CYANOBACTERIUM
SYNECHOCYSTIS PCC 6803**

PhD Thesis

Submitted by

Sandeesh Kodru

Supervisor: Prof. Dr. Imre Vass

Biological Research Center

Institute of Plant Biology

Laboratory of Molecular Stress and Photobiology



In partial fulfillment of the requirements

For the Degree of Doctor of Philosophy

Faculty of Science and Informatics, University of Szeged,

Szeged, Hungary

2021

Preface

This thesis is based on a research project whose aim is to obtain a better understanding of electron transport properties, which are related to the photodamage and photoprotection of the Photosystem II complex of the photosynthetic apparatus in the model organism *Synechocystis* PCC 6803. The project was carried out in the laboratory of Dr. Imre Vass, Director of the Institute of Plant Biology, Biological Research Center, Szeged, Hungary. This thesis work is supported by the Hungarian Ministry for National Economy (GINOP-2.3.2-15-2016-00026) and National Research, Development and Innovation Office (K-116016).

DEDICATION

*This thesis is dedicated to my beloved parents who
have always been a source of loving, inspiration and encouragement
to undertake my higher studies and face eventualities of life
with zeal, enthusiasm and fear of God*

Table of Contents

1. Introduction and literature review	7
1.1. The process of photosynthesis in general	7
1.2. Cyanobacteria as model organisms.....	8
1.3. Major complexes of the primary photosynthetic processes	9
1.3.1. Structure of phycobilisome	9
1.3.2. Photosystem II.....	10
1.3.3. Cyt b ₆ f complex.....	10
1.3.4. Photosystem I.....	11
1.3.5. ATP synthase.....	12
1.4. Linear and cyclic electron transport pathways	12
1.5. Alternative electron transfer pathways	13
1.6. Organization, composition and structure of Photosystem II.....	13
1.7. Effects of high light stress on Photosystem II	15
1.8. Generation of ROS in the photosynthetic apparatus and their involvement in photodamage	16
1.8.1. Production of superoxide in the photosynthetic apparatus.....	17
1.8.2. Production of singlet oxygen in the photosynthetic apparatus.....	17
1.8.3. Monitoring photodamage in the presence of protein synthesis inhibitors	18
1.9. Afterglow TL phenomenon for studying CEF.....	19
2.0. Aims of the study	20
3.0 Materials and methods	20
3.1. <i>Synechocystis</i> cell cultures, growth conditions and pigment extraction.....	20
3.1.1. Chlorophyll content determination.....	21
3.1.2. Light induced oxygen uptake measurement in <i>Synechosystis</i> cells	21
3.1.3. Photoinhibitory treatment of <i>Synechocystis</i> cells.....	21
3.1.4. Statistical analysis	22
3.2. Thylakoid and PSII membrane preparation	22
3.2.1. Light-induced oxygen uptake measurement in thylakoid membranes and PSII particles	22
3.2.2. Photoinhibitory treatment of thylakoid and PSII membranes	22
3.3. Thermoluminescence measurements procedure	23
3.3.1 Measurement of chlorophyll fluorescence induction transients.....	23
4.0. Results and Discussion	24
4.1. Chloramphenicol mediates an alternative electron transfer pathway in PSII isolated thylakoid membrane particles, which results in superoxide production and superoxide-induced photodamage	24
4.1.1. Production of O ₂ ^{•-} by chloramphenicol in isolated spinach thylakoid	24

4.1.2. Production of superoxide by chloramphenicol in isolated PSII particles	28
4.1.3. Chloramphenicol acts as electron acceptor in PSII.....	30
4.1.4. Conclusions concerning the effects of CAP on PSII electron transport and photodamage in isolated thylakoids and PSII membrane particles.....	32
4.2. Effect of chloramphenicol on photodamage of intact WT and PSI-less <i>Synechocystis</i> cells	33
4.2.1. Effect of chloramphenicol on the extent of PSII photodamage in WT <i>Synechocystis</i> cells.....	33
4.2.2. Effect of lincomycin and chloramphenicol concentration on PSII photodamage and recovery in WT <i>Synechocystis</i>	35
4.2.3. Chloramphenicol enhances PSII photodamage in comparison to lincomycin in PSI-less <i>Synechocystis</i>	38
4.2.4. Effect of photoheterotrophic growth on photoinhibitory activity loss in WT <i>Synechocystis</i> cells	39
4.2.5. Chloramphenicol induces oxygen uptake in WT and PSI-less <i>Synechocystis</i> cells	41
4.2.6. Conclusions concerning the effects of chloramphenicol on PSII electron transport and photodamage in intact WT and PSI-less <i>Synechocystis</i> cells.....	43
4.2.6.1. Chloramphenicol enhances PSII photodamage in intact <i>Synechocystis</i> cells	43
4.2.6.2. PSII photodamage is enhanced in the absence of PSI.....	43
4.2.6.3. Chloramphenicol should be used with caution in photoinhibition studies.....	44
4.3. Characterization of cyclic electron transport in <i>Synechocystis</i> by measuring the AG TL band.....	45
4.3.1. A +40 °C TL component with AG band characteristics is observed in low CO ₂ -grown <i>Synechocystis</i> cells	46
4.3.2. Temperature dependence of the TL curves of far-red light illuminated <i>Synechocystis</i> cells	49
4.3.3. The 40 °C TL band is missing in the M55 mutant that lacks NDH-1-mediated cyclic electron flow	51
4.3.4. Post-illumination fluorescence rise is connected with the appearance of the +40 °C TL band	52
4.3.5. Conclusions about the origin of the AG band and its connection with NDH-1 mediated CEF.....	53
5.0. Bibliography.....	55
6.0. Summary	77
7.0. Összefoglalás	79
8.0. LIST OF PUBLICATIONS	81
<i>Acknowledgements</i>	83

List of figures

Fig. 1.1. Schematic model of cyanobacterial thylakoid membrane electron transport	8
Fig. 1.2. Schematic structure of the phycobilisome (PBS) light-harvesting complex in the cyanobacterium <i>Synechocystis</i> sp. PCC 6803	9
Fig. 1.3. Schematic model of structural organization of PSII within thylakoid membrane.....	14
Fig. 4.1.1. The effect of chloramphenicol and SOD on the rate of oxygen uptake in spinach thylakoid.....	25
Fig. 4.1.2. Effect of chloramphenicol on the extent of light induced PSII photodamage in spinach thylakoid membranes	26
Fig. 4.1.3. The effect of chloramphenicol addition on PSII activity in spinach thylakoid membranes as quantified by fast chlorophyll fluorescence rise	27
Fig. 4.1.4. Concentration dependence of chloramphenicol addition on PSII activity in spinach thylakoid membranes as quantified by changes in variable fluorescence and F_v/F_m	28
Fig. 4.1.5. The effect of chloramphenicol and SOD on the rate of oxygen uptake in spinach BBY.....	29
Fig. 4.1.6. The effect of chloramphenicol addition on PSII activity in BBY membranes as quantified by fast chlorophyll fluorescence rise.....	30
Fig. 4.1.7. Photosynthetic activity of spinach PSII membranes was assessed by measuring OJIP transients of chlorophyll fluorescence... ..	31
Fig. 4.2.1. Impact of chloramphenicol on the extent of light-induced PSII photodamage in <i>Synechocystis</i>	34
Fig. 4.2.2. Effect of concentration of lincomycin on the rate of photodamage.....	35
Fig. 4.2.3. Effect of lincomycin and chloramphenicol concentration on PSII photodamage and recovery.....	36
Fig. 4.2.4. Differential effects of lincomycin and chloramphenicol on photoinhibitory activity loss in PSI-less <i>Synechocystis</i> cells.....	39
Fig. 4.2.5. Effect of glucose on the photoinhibitory effect on WT <i>Synechocystis</i> cultures.....	40
Fig. 4.2.6. Differential light sensitivity of WT and PSI-less <i>Synechocystis</i> cell.....	41
Fig. 4.2.7. Effect of CAP on the rate of oxygen evolution in <i>Synechocystis</i> cells.....	42
Fig. 4.2.8. The scheme illustrates the production of superoxide via PSI and PSII by chloramphenicol and in consequence damages PSI.....	45
Fig. 4.3.1. TL curves low CO ₂ -grown WT <i>Synechocystis</i> cells.....	46
Fig. 4.3.2. TL curves measured after FR illumination of high CO ₂ -grown WT cells.....	47
Fig. 4.3.3. Identification of individual components in the thermoluminescence (TL) curves of far-red (FR)-illuminated <i>Synechocystis</i> cells by curve resolution	48
Fig. 4.3.4. Temperature dependence of the inducibility of the AG band in <i>Synechocystis</i> cells	50
Fig. 4.3.5. Thermoluminescence curves of M55 mutant <i>Synechocystis</i> cells	51
Fig. 4.3.6. Variable chlorophyll fluorescence transients of <i>Synechocystis</i> cells	52
Fig. 4.3.7. Scheme of the AG band formation in cyanobacteria	54

List of Tables

Table 1. Rates of PSII photodamage.....	37
---	----

LIST OF ABBREVIATIONS

ATP– Adenosine triphosphate	PQ – Plastoquinone
AG – After glow	Q _A – Primary quinone electron acceptor
Chl – Chlorophyll	Q _B –Secondary quinone electron acceptor
¹ Chl*–Singlet excited state	SOD– Superoxide dismutase
³ Chl*– Triplet excited state	TE– Terminal emitters
CEF – Cyclic electron flow	TL– Thermoluminescence
CAP – Chloramphenicol	Tyr _Z – Tyrozine-Z
Cyt- <i>b₆f</i> – Cytochrome <i>b₆f</i> complex	Tyr _D – Tyrozine-D
DMBQ– 2, 6- Dimethoxy-1, 4-benzoquinone	Xe– Xenon
DCMU– 3, 4-dichloro-1, 1-dimethyl urea	
DNA– Deoxyribonucleic Acid	
Fd– Ferredoxin	
FR – Far-red illumination	
F _m – Maximum fluorescence in dark	
F _o – Minimum fluorescence	
F _v /F _m – Maximum quantum yield	
LEF– Linear electron flow	
LHCI – Light-harvesting complex I	
LHCII – Light-harvesting complex II	
NPQ – Non-photochemical quenching	
NDH– NAD(P)H dehydrogenase	
NADPH– Nicotinamide adenine dinucleotide phosphate	
PSI– Photosystem I	
PSII– Photosystem II	
ROS– Reactive oxygen species	
PAR– Photosynthetically active radiation	
PQH ₂ – Plastoquinol	
PGR5- Proton gradient regulation 5	
PC– Plastocyanin	
Phe– Pheophytin	
P680 – reaction center chlorophyll of PSII	
P700 – reaction center chlorophyll of PSI	

1. Introduction and literature review

1.1. The process of photosynthesis in general

Photosynthesis is the process that supports complex life on earth - all of the oxygen on our planet comes from photosynthesis. There are two types of photosynthesis: oxygenic and anoxygenic. Oxygenic photosynthesis, which is performed by cyanobacteria, algae and plants utilizes the energy of light to split water molecules, releasing oxygen, electrons and protons in the process. Anoxygenic photosynthesis, which is performed by photosynthetic bacteria uses compounds such as hydrogen sulfide, or hydrogen, or ferrous ion (Peretó 2011) rather than water, as electron donors, and it does not produce oxygen. In oxygenic photosynthesis, light energy is utilized to produce organic compounds, mainly sugars, which are used as a fuel for all metabolic processes of the organisms. This is a highly regulated multi-step process which includes the harvesting of solar energy, the transfer of excitation energy, energy conversion and electron transfer from water to NADP^+ , generation of ATP and enzyme reactions, which assimilate carbon dioxide and synthesize carbohydrates.

In a series of reactions beginning with the excitation of chlorophylls in the light-harvesting complexes LHCI and LHCII, light energy is converted in the chloroplasts into chemical energy by two different functional units referred to as photosystems. The light energy is also used to generate the driving force of the protons through the thylakoid membrane that is utilized to generate ATP (Mitchell et al., 1961).

Light (Photosynthetically active radiation, PAR, 400-700 nm) is the driving force for oxygenic photosynthesis. Light is absorbed by chlorophyll and carotenoid pigment molecules in all photosynthetic systems, as well as by phycobilins in cyanobacteria. When light is absorbed by chlorophyll, it is converted into the first singlet excited state ($^1\text{Chl}^*$). The excitation energy may be (1) used to conduct the photochemistry, (2) re-emitted in the form of fluorescence, (3) dissipated in the form of heat (NPQ), or (4) the singlet excited state can be dissipated via the chlorophyll triplet ($^3\text{Chl}^*$), which can produce reactive oxygen species (ROS) as by-products.

The net equation of photosynthesis:



The transformation of CO_2 into $\text{C}_6\text{H}_{12}\text{O}_6$ (glucose) occurs primarily in the Calvin-Benson-Bassham cycle, requiring NADPH and ATP as co-factors. These co-factors are generated during a complex reaction series involving light capture, electron transport, water

splitting and proton pumping. The photosynthetic apparatus, as depicted in Fig. 1.1, contains four pigment-protein complexes embedded in the thylakoid membrane, known as Photosystem I (PSI), Photosystem II (PSII), Cytochrome b_6/f and ATP synthase (Scherer 1990).

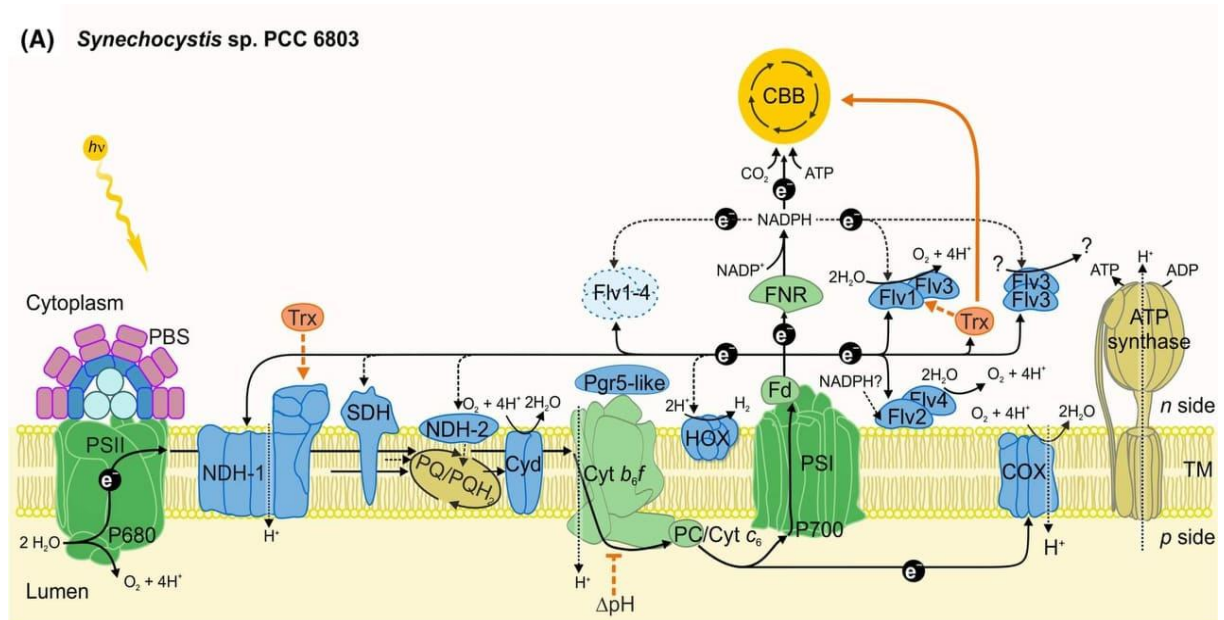


Fig.1.1. Schematic model of cyanobacterial thylakoid membrane electron transport (Nikkanen et al. 2021)

1.2. Cyanobacteria as model organisms

Cyanobacteria, formerly known as blue-green algae, were one of the first eubacteria to evolve more than 2.5 billion years and have strongly influenced the terrestrial biosphere (Falkowski 2006; Schirmer et al. 2015). Cyanobacteria have also played a major role in early biogeochemical processes, and in the evolution and oxygenation of life and land (Demoulin et al., 2019). They play an important role in food webs as primary producers of biomass (Blankenship 1992). Cyanobacteria are photooxygenic bacteria responsible for a significant portion of primary productivity and nitrogen fixation. *Synechocystis* sp. PCC 6803 has been one of the most popular organisms for genetic and physiological studies of photosynthesis for two major reasons; it is naturally transformable by exogenous DNA and grows heterotrophically at the expense of glucose. *Synechocystis* sp. PCC 6803 was the third prokaryote and first photosynthetic organism whose genome was completely sequenced (Kaneko et al. 1996). Databases supporting *Synechocystis* research are CyanoBase (<http://genome.kazusa.or.jp/cyanobase/Synechocystis/>) which provides an easy way of accessing the sequences and all-inclusive annotation data on the structures of the

cyanobacterial genomes. STRING (<https://string-db.org/>) is a database of known and predicted protein-protein interactions.

SynechoNET (<http://biportal.kobic.re.kr/SynechoNET/>) is an integrated protein-protein interaction database. cTFbase (<http://bioinformatics.zj.cn/cTFbase/index.php>) retrieve all TF sequences and their detailed annotation information, including sequence features, domain architecture and sequence similarity against the linked databases.

1.3. Major complexes of the primary photosynthetic processes

1.3.1. Structure of phycobilisome

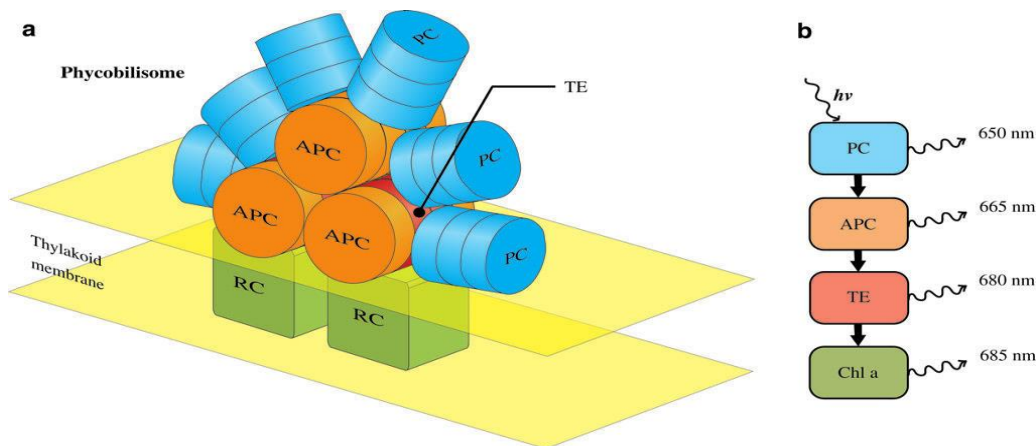


Fig.1.2. Schematic structure of the phycobilisome (PBS) light-harvesting complex in the cyanobacterium *Synechocystis sp. PCC 6803* (Dartnell et al. 2011)

Cyanobacteria and red algae are two important groups of photosynthetic organisms which possess a light-harvesting antenna complex known as phycobilisomes (PBS) (Croce et al., 2014). Phycobilisomes are macro-molecular structures attached to the stromal surface of the thylakoid membranes. They absorb light energy and transfer it to the PSI and PSII reaction centers (Liu et al. 2013). In cyanobacteria, there are 3 main types of phycobiliproteins: phycoerythrin (PE), phycocyanin (PC) and allophycocyanin (APC) (Yamanaka et al. 1978; Mimuro et al. 1999; Nobel 2005). The PBS TE (terminal emitters) is the lowest energy state in the PBS antenna system that funnels excitation energy into the reaction centre of PSII. APCs have a major absorption peak of approximately 650 nm, and their emission peak is approximately 660 nm, while PCs absorb between 610 and 635 nm and have fluorescence limits between 635 and 648 nm. Moreover, allophycocyanin-B (AP-B) has maximum

absorption at approximately 650 nm with a shoulder at 675 nm, and has emission bands at 660 nm, and about 680 nm (Bryant et al. 1979).

1.3.2. Photosystem II

PSII is a large, 700 kDa homo-dimeric, membrane protein complex situated within the thylakoid membranes of organisms ranging from cyanobacteria to higher plants. Cyanobacterial PSII contains 20 subunits, of which 17 are transmembrane and 3 are membrane-peripheral extrinsic subunits (Shen et al. 2008). Each PSII monomer is made up of a core complex and a peripheral complex. The core complex is made up of D1 and D2 subunits, bound by the antenna subunits CP43 and CP47. The D1 and D2 subunits form the backbone of the reaction centre, while the CP43 and CP47 subunits bind chlorophylls that absorb light energy and transfer it to the D1/D2 reaction centre (Barber et al. 2002). The 3 membrane-peripheral, extrinsic proteins are associated with the luminal side of PSII, where the water-splitting reaction takes place. The cluster of reaction center Chls in PSII is referred to as P680; it comprises four Chls bound to the D1 and D2 subunits (Raszewski et al. 2008; Renger and Renger 2008; Yamanaka et al. 2011). Upon absorption of light energy, one of the Chls becomes excited and donates one electron to the initial electron acceptor pheophytin, which transfers the electron to the primary and secondary plastoquinone acceptors, Q_A and Q_B . The oxidized P680 is reduced by a nearby tyrosine residue, Tyr161 of the D1 subunit, designated as Y_Z (Barry and Babcock 1987; Debus et al. 1988), which in turn oxidizes a Mn_4CaO_5 cluster, which is the catalytic center for water splitting. When the four electrons have been extracted from the Mn_4CaO_5 cluster, two water molecules are split into four protons and one oxygen molecule. Thus, water-splitting is a four-electron reaction that occurs through the S_i -state cycle, where $i = 0-4$ (the so-called Kok cycle) (Joliot 2003; Kamiya and Shen 2003). S_0 is the most reduced state, whereas S_1 is dark stable, and oxygen is produced during the $S_3-(S_4)-S_0$ transition. S_0 is oxidized gradually in the dark by Y_D^+ , a Y_Z analog a redox-active tyrosine residue of the D2 subunit (D2-Tyr160) (Styring and Rutherford 1987; Styring et al. 2012). PSII also contains carotenoid pigments, which are involved in light harvesting, photoprotection, protection against singlet oxygen, excess energy dissipation and structure stabilization (Bialek-Bylka et al. 1998).

1.3.3. Cyt b_6f complex

Cyt b_6f is a ~220 kDa functional dimer made up of four major subunits: cytochrome f (cyt_f) (PetA), Cytochrome b_6 (Cyt b_6) (PetB), the Rieske iron-sulphur protein (PetC) and subunit IV (PetD), as well as four minor subunits (Pet G, L, M, N). Cytochrome b_6f (Cyt b_6f)

serves as a link between photosystem II (PSII) and photosystem I (PSI) through the oxidation and reduction of the plastoquinol (PQH₂) and plastocyanin (PC) electron carriers. Cyt b₆f couples electron transfer between PSI and PSII to the generation of proton motive force via the Q-cycle (Mitchell 1975; Crofts et al. 1983) where one of the electrons from PQH₂ enters into the linear electron transport chain through PSI while the other flows back to the PQ pool via a cyclic pathway. An important function of Cyt b₆f is to attenuate the formation of ROS by avoiding short-circuits of the Q-cycle and mitigating superoxide production (Osyczka et al. 2005; Cape et al. 2006). Cyt b₆f is the site of the rate-limiting step in linear electron transfer and is downregulated by Δp^H to protect PSI from damage.

The redox-active cofactor of plastocyanin (PC) molecule is a copper protein that transfers electrons from Cyt b₆f to PSI. In some cyanobacteria Cyt c₆ is present instead of PC (Torrado et al., 2019). Such small, water-soluble electron-carrier proteins play a ubiquitous role in both respiratory and photosynthetic electron transfer chains by carrying electrons between integral membrane complexes (Hope 2000).

1.3.4. Photosystem I

Photosystem I is a large multi-unit protein complex, embedded in the thylakoid membrane. PSI consists of 12 protein subunits (cyanobacteria) and 13 subunits (plant systems) encoded by the *psaA* to *psaX* genes. PSI in cyanobacteria exists in the photosynthetic membrane in trimeric, tetrameric and oligomeric form (Li et al. 2019). Photosystem I of cyanobacteria contains an integral antenna system consisting of about 90 Chl a molecules and 22 carotenoids, three [4Fe-4S] clusters and two phylloquinones. These chlorophylls belong to the antenna system of PSI and are used to capture the light energy. In PSI, the P700 chlorophyll dimer is the primary electron donor, which in its excited state (P700*) transfers an electron to the primary electron acceptor A₀ (Chl a molecule), A₁ (a phylloquinone molecule) and from there subsequently to the iron-sulfur clusters, F_X, F_A and F_B. The latter mediates electron transfer to ferredoxin, which act as soluble electron carrier. Ferredoxin transfers the electron to the ferredoxin NADP⁺-reductase enzyme (FNR), which then finally reduces NADP⁺ to NADPH (Chitnis 2001). On the donor side of PSI P700⁺ is re-reduced by plastocyanin (PC) or Cyt c₆ (in cyanobacteria), which delivers electrons from the cyt b₆f complex. NADPH, together with ATP, is used to reduce CO₂ to carbohydrates in the subsequent dark reactions (Fromme et al. 2001).

1.3.5. ATP synthase

ATP synthase is the very last enzyme in the oxidative phosphorylation pathway that makes use of electrochemical energy to power ATP synthesis. During proton translocation through the thylakoid membrane, which is coupled to photosynthetic electron transport, the stroma becomes alkaline and the lumen becomes acidic. The proton gradient creates a proton motive force for ATP synthesis. ATP synthase is made up of a hydrophobic part (CF₀), which forms a channel allowing the passage of protons through the membrane and a part that protrudes into the stroma (CF₁) and is formed by several peptides. The activity of the ATP synthase regulates the flux of oxidative phosphorylation (Boyer 1997), execution of cell death (Sánchez-Cenizo et al. 2010; Sánchez-Aragó et al. 2013) and mitochondrial signaling by reactive oxygen species (Formentini et al. 2012; Martínez-Reyes and Cuezva 2014).

1.4. Linear and cyclic electron transport pathways

Photosynthesis operates in two modes of electron transport, linear and cyclic. In the linear pathway (LEF), electrons from the oxidation of water are passed from the reaction centre of PSII to the Q_A/Q_B electron acceptors. The electrons are then transferred into the PQ pool located in the lipid phase of the thylakoid membrane. This is then coupled to electron donation to the Q₀ site of the cytochrome b₆/f complex. The electron-coupled proton translocation generates a proton motive force across the thylakoid membrane that is used by the CF₁-F₀ ATP synthase to form ATP. In the linear mode, the electron transfer at the acceptor side of PSI proceeds via Fd and ferredoxin-NADP⁺-oxidoreductase (FNR) to reduce NADP⁺, generating NADPH. Photo-produced ATP and NAD(P)H then allow CO₂ fixation by the Calvin-Benson-Bassham cycle and other metabolic processes.

In the cyclic configuration part of the electrons can return from the acceptor side of PSI to the PQ pool, thereby creating a cyclic flow of electrons (CEF) around PSI. There are two main CEF pathways: (i) the NADH dehydrogenase-like complex-dependent pathway (NDH-CEF); (Shikanai et al. 1998; Burrows et al. 1998; Kofer et al. 1998; Yamamoto et al. 2011) and the ferredoxin-plastoquinone reductase pathway (FQR-CEF); (Munekage et al. 2002; DalCorso et al. 2008). The NDH-1 complex accepts electrons from ferredoxin (Fd) or NAD(P)H at the PSI acceptor side, and transfers them to Cyt b₆/f through PQ reduction (Peltier, Aro, and Shikanai 2016), (Strand, Fisher, and Kramer 2017). In cyanobacteria, the NDH-1 appears to be the major protein complex involved in CEF. One NDH-1 subunit of the hydrophilic domain, Ndhs, is responsible for interacting with ferredoxin and initiating CEF (Battchikova et al. 2011c; He et al. 2015; Schuller et al. 2019). FQR-CEF involves the Cyt

b₆/f complex, plastocyanin, PSI, ferredoxin (Fd) and ferredoxin plastoquinone reductase FQR. PGR5 was identified as an essential component of the FQR-CEF (Munekage et al. 2002).

The main difference between the two types of electron transport pathways is that the LEF generates both ATP and NADPH, while CEF is exclusively involved in ATP synthesis without the accumulation of NADPH. The CEF pathway also protects the photosynthetic machinery when there is an imbalance between the production of excited electrons and their consumption and regulates the ratio between ATP and NADPH produced.

The main function of CEF-PSI is the enhancement of photoprotective NPQ, through generating the electrochemical potential difference across the thylakoid membrane (Munekage et al. 2002).

1.5. Alternative electron transfer pathways

Besides the main linear and cyclic electron transport pathways further, alternative routes of photosynthetic electron transport also exist. Pseudo-cyclic electron flow (PCEF) results in the reduction of oxygen to water by the Mehler reaction (Mehler-PCEF) during which reactive oxygen species (ROS) are generated and scavenged (Leister 2019). PSI directly oxidizes O₂ to form O₂^{•-}, which is then converted first into hydrogen peroxide (H₂O₂) and finally to O₂ and water by superoxide dismutase (SOD) and ascorbate peroxidase in Mehler reaction (Asada et al. 2000). The water-water cycle (WWC) acts as a large electron sink (Asada et al. 2000) and generates the electrochemical potential difference of H⁺ across the thylakoid membrane, which enhances the non-radiative dissipation of excess light energy through non-photochemical quenching NPQ (Asada 1999; Asada et al. 2000; Miyake 2010). The CEF-PSI and WWC are thought to protect plants from damage that occurs due to the over-reduction of the thylakoids under stress conditions (Miyake 2010).

In cyanobacteria, there is a Mehler-like reaction, which can reduce O₂ with electrons mediated by PSI by means of soluble flavodiiron proteins 1 and 3 (Allahverdiyeva et al. 2011, 2013; Alboresi et al. 2019; Santana-Sánchez et al. 2019). It is a four-electron transfer reaction and it does not produce ROS and may protect PSI against the production of O₂^{•-} (Allahverdiyeva et al. 2013).

1.6. Organization, composition and structure of Photosystem II

PSII complexes in chloroplast are primarily located in stacked thylakoid-grana, while the PSI complexes are located in the non-stacked thylakoid region, referred to as lamella (Albertsson 2001a, b; Rast et al. 2015; Pribil et al. 2018).

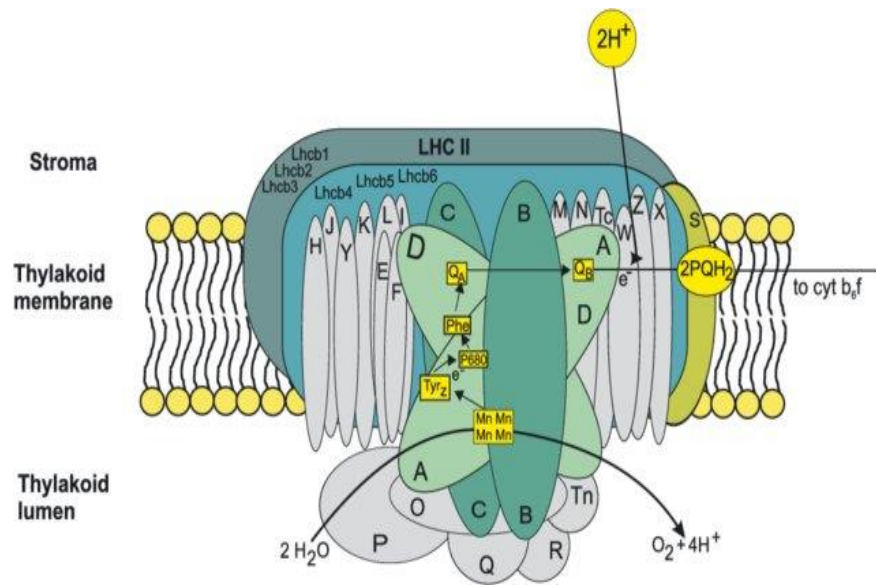


Figure 1.3. Schematic model of structural organization of PSII within thylakoid membrane. (Luciński and Jackowski 2006)

PSII components include core proteins, low-molecular-mass proteins, extrinsic oxygen-evolving complex (OEC) proteins, and light-harvesting complex (LHC) proteins (Liu et al. 2004; Aro et al. 2005; Umena et al. 2011). The core of the PSII includes four transmembrane protein subunits: D1 (PsbA), D2 (PsbD), CP43 (PsbC) and CP47 (PsbB). Reaction center proteins D1 and D2 consist mainly of closely interconnected transmembrane propellers for structural stability, pigment and cofactor binding, and scaffolding for electron carriers. The four transmembrane proteins bind Chl a, beta-carotene and non-heme iron, and transfer the excitation energy absorbed by pigments of peripheral light-harvesting proteins to the reaction center. These four major subunits are present in higher plants, cyanobacteria and red algae. In addition, there are hydrophilic extrinsic proteins (PsbO, PsbP, PsbQ, and PsbTn), intrinsic subunits (PsbE, PsbF, PsbH, PsbI, PsbJ, PsbK, PsbL, PsbM, PsbT_C, PsbW, PsbX, and PsbZ). PsbE and PsbF are the subunits of Cytb₅₅₉. These subunits are expected to participate in the protection of PSII against photodamage (Nixon et al. 2005; Mulo et al. 2008). The extrinsic proteins PsbO, PsbP and PsbQ, stabilize the OEC. OEC acts as the active site for water oxidation. The PSII-light-harvesting antenna (i.e., light-harvesting complex II, abbreviated as LHCII) in land plants is an integral membrane complex. LHCII contains three major trimeric PSII light-harvesting chlorophyll a/b-binding (LHCB) proteins LHCB1, LHCB2, and LHCB3 and three minor monomeric LHCB proteins LHCB4, LHCB5, and LHCB6 (Liu et al. 2004). Light energy is harvested in cyanobacteria by chlorophyll-

containing photosystems embedded in the thylakoid membranes and phycobilisomes (PBSs), photosystem-associated light-harvesting antennae.

1.7. Effects of high light stress on Photosystem II

Even though light is the source of energy for the photosynthetic processes it can also cause damage to plants and algae. Excess light reaching the photosynthetic apparatus can cause photodamage and ultimately can lead to the death of photosynthetic organism (Arntzen et al. 1984; Aro et al. 1993a; Vass and Aro 2008; Zavafer et al. 2017). High light leads to the inactivation of PSII and results in damage to the reaction center, mainly the D1 protein subunit (Prasil et al. 1992; Sass et al. 1997). This stress situation is known as photoinhibition (Ögren and Sjöström 1990). The damaged Photosystem II complex dissociates from the light-harvesting antenna and migrates from appressed to non-appressed thylakoid regions where a new D1 protein is co-translationally inserted into the partially disassembled photosystem II complex. The '32kDa-Q_B binding protein', now known to be the D1 protein, of the PS II reaction center was suggested to be involved in the photoinhibition process (Kyle et al. 1984; Ohad et al. 1984). PSII photochemistry is downregulated, resulting in decreased photosynthetic performance and reduced growth and productivity (Chen et al. 2017).

In living organisms, photoinhibited PSII centers are continuously repaired via degradation and synthesis of the D1 protein of the photosynthetic reaction centre of PSII. The repair mechanisms of PSII consists of several steps, which involves partial disassembly of damaged complexes including proteolytic degradation of the D1 protein using FtsH (FtsH2 and FtsH3) and Deg proteases (Nixon et al. 2010), synthesis of the precursor to the D1 protein (pre-D1), insertion of the newly synthesized precursor into the thylakoid membrane with the assembly of other PSII proteins, maturation of the D1 protein by C-terminal processing of pre-D1; and assembly of the oxygen-evolving machinery (Aro et al. 1993a; Chow and Aro 2005; Murata et al. 2007). A large amount of ATP is required for the repair of PSII, both ATP and the reduced and activated forms of translational elongation factors are critical factors in the synthesis of the D1 protein (Zhang et al. 2000; Murata and Nishiyama 2018). The repair rate for PSII may also be affected by several environmental factors. Salt, cold, moderate heat, oxidative stress and CO₂ limitation can all inhibit PSII repair and thus enhance photodamage (Tyystjärvi and Aro 1996; Anderson and Chow 2002; Allakhverdiev and Murata 2004; Murata et al. 2007). A previous study has shown that regulation of PSII photoinhibition is the essential controller of the photosynthetic electron transfer chain which provides

photoprotection against ROS formation and photodamage in PSI (Tikkanen and Aro 2014). Therefore the balance of photodamage and repair determines the extent of photoinhibition.

The importance of photodamage is emphasized by the large array of mechanisms that protect plants against the detrimental effects of light. These include: (i) dissipation of excess light energy in the antenna (Demmig et al. 1988; Owens 1996; Müller et al. 2001; Ivanov et al. 2008b; Karapetyan 2008; Dall'Osto et al. 2017) or the PSII reaction center (Ivanov et al. 2008a) before photosynthetic electron transport occurs; (ii) quenching of dangerous Chl triplets and singlet oxygen (Fiedor et al. 2005; Krieger-Liszkay 2005; Telfer 2005, 2014), and (iii) repair of the damaged PSII complexes via *de novo* synthesis of the D1 reaction center protein (Aro et al. 1993c; Sass et al. 1997; Komenda et al. 2007).

The rate coefficient of photodamage is directly proportional to light intensity, and this relationship holds under strong and weak light (Tyystjärvi and Aro 1996; Anderson and Chow 2002; Allakhverdiev and Murata 2004; Murata et al. 2007). Photoinhibition can be caused by ultraviolet (UV) and visible light (V), and by the interaction of UV-V (Powles 1984; Sicora et al. 2003). Photoinhibition occurs under a wide range of light intensities of visible (400-700 nm) and ultraviolet light (220-400 nm) (Vass et al. 1996). The damaging effect of UV-A radiation (315-400 nm) is very similar to UV-B (Vass et al. 2002).

1.8. Generation of ROS in the photosynthetic apparatus and their involvement in photodamage

The effects of ROS on photodamage to PSII and on repair have been investigated in depth both in cyanobacterial cells and in intact leaves. In plant cells the major source of ROS production are the chloroplast and mitochondria (Apel and Hirt 2004). ROS are small molecules derived from oxygen molecules including free oxygen radicals, such as superoxide ($O_2^{\cdot-}$) (Chen et al. 1992), hydroxyl (OH^{\cdot}), peroxy (RO_2^{\cdot}) (Miyao et al. 1995) and alkoxy (RO^{\cdot}) as well as hypochlorous acid (HOCl), ozone (O_3), singlet oxygen (1O_2), and hydrogen peroxide (H_2O_2), which are non-radicals (Nishiyama et al. 2005). These species are produced when cells are subjected to stress conditions.

ROS generation may induce photooxidative damage by: (i) induction of D1 protein degradation, and (ii) inhibition of D1 protein *de novo* synthesis during photoinhibition (Lee et al., 2013). There are two main mechanisms proposed for the photoinhibition of PSII: acceptor-side and donor-side photoinhibition (Barber and Andersson 1992; Aro et al. 1993a; Yamamoto et al. 1999). Photodamage related to triplet chlorophyll formation and singlet excited oxygen (1O_2) formed is thought to be responsible for the photodamage of PSII in acceptor-side photoinhibition (Vass et al. 1992; Telfer et al. 1994; Hideg et al. 1998; Vass

2011, 2012a; Rehman et al. 2013). Donor-side mediated photodamage occurs in the presence of a functionally impaired water oxidizing complex. Donor-side photoinhibition involves cationic radicals like P680⁺ and Tyr_Z⁺ causing damage to D1 protein (Jegerschöld et al. 1990; Blubaugh et al. 1991).

Abiotic stress accelerates the generation of ROS. ¹O₂ is a form of molecular oxygen, with singlet electron spin configuration, which is extremely reactive (Ogilby 2010). It attacks and oxidizes proteins, lipids and nucleic acid. Studies show that singlet oxygen formation is enhanced under high light conditions and consequently leads to PSII inactivation and ultimately photoinhibition (Vass et al. 1992; Aro et al. 1993b; Macpherson et al. 1993; Long et al. 1994; Komenda and Barber 1995; Melis 1999; Kruk et al. 2005; Krieger-Liszkay et al. 2008; Vass and Cser 2009; Vass 2012b, 2019). Under high light conditions, CO₂ limitation enhances photodamage. Under such conditions, the plastoquinone pool is in a reduced state, electron transport is limited and charge recombinations induce singlet oxygen formation.

1.8.1. Production of superoxide in the photosynthetic apparatus

Superoxide is produced in photosynthetic organisms by photo-reduction of oxygen via electron transport at the acceptor side of PSI (Asada et al., 2000). O₂^{•-} is moderately reactive with a short lifetime of 2-4 μs and a migration distance of 30 nm (Gechev et al. 2006) can induce damage to proteins and membrane components due to its ability to produce highly oxidizing radicals. Superoxide can act as either oxidant or reductant; it can oxidize sulfur, ascorbic acid or NADPH; it can reduce cytochrome c and metal ions (Gebicki and Bielski 1981). The superoxide radical is formed mainly in the thylakoid localized PSI during non-cyclic electron transport chain (ETC), as well as other cellular compartments. The major site of superoxide (O₂^{•-}) anion production is the Fe-S centres on the acceptor side of PSI (Flint, 1993), but it can also be produced in PSII (Pospíšil 2009). Superoxide radicals usually occur in their anionic form and are unable to permeate membranes. Superoxide is considered as an intermediate product of the water-water cycle or the Mehler reaction, associated with PSI (Asada 1999). In the presence of superoxide dismutase (SOD) superoxide is quickly dismutated to stable hydrogen peroxide (Fridovich 1997). O₂^{•-} formation has been suggested to occur in PSII during high light exposure in the absence of added electron transport mediators (Pospíšil 2009, 2012; Pospíšil et al. 2019).

1.8.2. Production of singlet oxygen in the photosynthetic apparatus

¹O₂ is produced via the interaction of the long-lived triplet excited state of pigment molecules, especially Chls. This can happen in the light-harvesting complexes, and also in

PSII. The absorption of light in the Chl containing light-harvesting complex (LHCII) and in the PSII complex leads to the excitation of the P680 reaction centre Chl. The charge separation between the excited reaction centre Chl assembly (P680*) and the primary electron acceptor pheophytin (Phe) molecule, i.e., the formation of the primary radical pair/charge-separated state (P680⁺Phe⁻), is a primary event during PSII electron transfer. This is further followed by rapid charge stabilization processes; the primary radical pair is stabilized by reduction of Q_A by Phe⁻ and oxidation of Tyr_Z by P680⁺ to prevent its rapid recombination. The P680⁺Phe⁻ state is initially formed in the singlet spin configuration ¹[P680⁺Phe⁻], which recombines to ¹P680* (Phe). However, spin conversion can convert ¹[P680⁺Phe⁻] to the triplet ³[P680⁺Phe⁻] state, whose recombination results in excited ³P680 (Phe). The interaction of the excited triplet ³P680 with the oxygen in the triplet ground state results in the formation of ¹O₂. The P680 triplet lifetime ranges from 1 ms in the presence of oxygen to 33 ms under anaerobic conditions (Durrant et al. 1990). Scavenging of triplet ³P680 from the place it formed takes place rapidly before ¹O₂ formation (Filatov et al. 2016).

1.8.3. Monitoring photodamage in the presence of protein synthesis inhibitors

Light stress to PSII becomes a problem when the rate of photodamage exceeds the rate of repair processes. Therefore, it is important to monitor separately the rates of photodamage and of the protein synthesis-dependent repair. Decoupling of photodamage and repair can be achieved by protein synthesis inhibitors, such as lincomycin or chloramphenicol, which block the initiation of protein synthesis and of peptide bond formation, respectively. Lincomycin is a specific inhibitor of chloroplast translation (Mulo et al., 2003). While there are no reports concerning the participation of lincomycin in photosynthetic electron transport, chloramphenicol has been reported to accept electrons from the acceptor side of Photosystem I and to transfer them to molecular oxygen leading to superoxide production (Okada et al. 1991). Although O₂^{•-} has lower reactivity than other ROS, it can induce damage to proteins and membrane components due to its ability to produce highly oxidizing radicals (Pospíšil, 2019). This side effect of chloramphenicol has been considered as a source of a potential artifact by several research groups, who used lincomycin instead of chloramphenicol in photoinhibition studies (Tyystjärvi and Aro 1996; Campbell and Tyystjärvi 2012; Tikkanen et al. 2014). However, other groups kept using chloramphenicol in measurements of PSII photodamage, which was contradictory to those studies in which lincomycin was used (Nishiyama et al. 2005; Takahashi and Murata 2005). It should be noted that chloramphenicol was used at 30–65 or 100 µg mL⁻¹ (Komenda and Masojídek 1998; Komenda et al. 1999;

Saradhi et al. 2000) in some early investigations, but it was applied at $200 \mu\text{g mL}^{-1}$ or higher concentrations in the majority of photosynthesis studies (Nishiyama et al. 2004; Takahashi et al. 2010, 2013; Inoue et al. 2011).

1.9. Afterglow TL phenomenon for studying CEF

Thermoluminescence (TL) provides a powerful tool to monitor the recombination reactions of oxidized donors and quinone acceptors of PSII leading to light emission. The technique is simple, inexpensive, and yet powerful in probing PSII in PSII enriched membranes and thylakoids to intact leaves and whole cells of cyanobacteria or algae. The main redox components that participate in TL emission are the reduced forms of the Q_A and Q_B quinone electron acceptors, the S_2 and S_3 redox states of the water-oxidizing complex, Tyr_D and Tyr_Z . At the lumen-oriented oxygen evolving complex positive charges are stored as S_1 to S_4 states. The S_0 and S_1 are stable in the dark and cannot recombine with Q_A^- or Q_B^- . S_4 is unstable as it produces an O_2 molecule, only S_2 and S_3 can recombine with PSII acceptor side components resulting in luminescence emission.

The afterglow (AG) thermoluminescence band, peaking around 45°C , originates from heat-induced back transfer of electrons from stroma to the acceptor side of PSII to Q_B in $S_{2/3}Q_B$ centers which creates the $S_{2/3}Q_B^-$ state (Sundblad et al. 1990; Miranda and Ducruet 1995; Havaux 1996; Ducruet et al. 2005). The AG band might be regarded as an indicator of changes in the levels of ATP and/or NADPH in the stroma (Krieger et al. 1998). However, the mechanism of afterglow emission is a complex phenomenon that requires reverse electron flow through $S_{2/3}Q_B$ centers and facilitated by the cyclic electron flow (García-Calderón et al. 2019; Ortega and Roncel 2021). The AG band can be observed, or enhanced in photosynthetic materials by using FR $> 700 \text{ nm}$ irradiation (Roncel et al. 2007, 2016). FR light preferentially excites PSI which causes oxidation of the PQ pool. The reduction of PSI acceptor pool results in the back transfer of electrons to the PQ pool via CEF pathway(s), which leads to reduction of oxidized Q_B in $S_{2/3}Q_B$ centers and creates TL precursor state. In addition to investigating the function of cyclic electron transfer pathways, AG band could also be used to investigate the effects of abiotic and biotic stress in chloroplasts (Janda et al. 2001).

The AG band is observed in *Arabidopsis thaliana* (Havaux et al. 2005), tobacco (Havaux et al. 2005) and *Chlamydomonas* (Ducruet et al. 2011), some unicellular microalgae, such as *Chlorella vulgaris* (Repetto et al. 2015), and *Phaeodactylum tricoratum* (Roncel et al. 2016). Although many investigators (Demeter and Govindjee 1989; Meetam et al. 1999;

Cser and Vass 2007; Cser et al. 2008) have observed TL from cyanobacteria, the AG component has not yet been found in these organisms (Havaux, 2005).

2.0. Aims of the study

The general aim of the project was to investigate the mechanism of photosynthetic electron transfer in isolated thylakoid membrane complexes, as well as cyanobacteria, to reach a better understanding of the mechanism of photoinhibition of PSII and cyclic electron flow around PSI.

The specific aims of this study were:

- 1, To understand the mechanisms of photodamage of the PSII complex in the presence of chloramphenicol in isolated thylakoid membrane particles and to investigate whether chloramphenicol has the capacity to interact directly with PSII electron transport in isolated membrane particles.
- 2, To understand light-induced PSII photoinhibition in WT *Synechocystis* and its PSI-less mutant in the presence of chloramphenicol and lincomycin and to understand the mechanisms of photodamage of the PSII complex in the presence of chloramphenicol in intact *Synechocystis* cells.
- 3, To obtain a better understanding of cyclic electron flow in cyanobacteria, by utilizing the potential of the AG thermoluminescence phenomenon and to test specific experimental conditions, which were expected to induce a temperature-dependent reduction of the PQ pool via CEF in *Synechocystis* 6803.

3.0 Materials and methods

3.1. *Synechocystis* cell cultures, growth conditions and pigment extraction

Synechocystis sp. PCC 6803 wild type and PSI-less mutant cells, obtained from Prof. Wim Vermaas (Shen Gaozhong et al. 1993), were grown autotrophically and photomixotrophically in BG-11 growth medium in a rotary shaker at 30 °C under a 3% CO₂-enriched atmosphere. The *Synechocystis* PSI-less mutant was grown in the presence of 25 µg mL⁻¹ spectinomycin and 5 mM glucose. As a control for the PSI-less strain, WT cells were also cultured under the same conditions, i.e., 5 µmol photons m⁻² s⁻¹ light intensity in the presence of 5 mM glucose when indicated. For thermoluminescence measurements WT

Synechocystis cells were propagated in BG-11 growth medium in a rotary shaker at 30 °C either at ambient air level CO₂, or under a 3% CO₂-enriched atmosphere. The M55 mutant (Δ ndhB, deficient in type I NADPH dehydrogenase complex, NDH-1) (Ogawa 1991; Cournac et al. 2004) of *Synechocystis* was grown under the same conditions as the WT (in 3% CO₂) in BG-11 medium supplemented with kanamycin (25 μ g mL⁻¹). 1 mL culture that had been kept at -80 °C was used as a starter culture. The *Synechocystis* cells were grown in 500 mL flasks containing 200 mL of BG-11. Cells in the exponential growth phase (A₅₈₀ of 0.8-1) were harvested by centrifugation at 8000 g for 10 min and re-suspended in fresh BG-11 medium at a concentration of 5 μ g of Chl mL⁻¹. The cells were kept under growth conditions for one hour in the incubator before measurement.

3.1.1. Chlorophyll content determination

The chlorophyll content of the *Synechocystis* cells was determined in methanol (100%). The absorption of each sample was determined at 650 nm and 665 nm using a spectrophotometer (UV-1601, Shi-madzu Corporation, Japan). Chl (a) concentration was calculated as:

$$\text{Chl (a)} = (16.5 \times A_{665} - 8.3 \times A_{650}) \times \text{dilution factor} \text{ (Dere S et al. 1998).}$$

The concentration was given in μ g/mL units.

3.1.2. Light induced oxygen uptake measurement in *Synechosystis* cells

Steady state O₂ evolution rates in wild-type *Synechosystis* and PSI-less mutant cells were measured with Hansatech DW₂ O₂ electrode at 30 °C under illumination of 2300 μ mole m⁻²s⁻¹ in the absence and presence of 200 μ g/mL chloramphenicol. The rate of O₂ uptake was calculated as the difference of the rates of O₂ evolution measured in the absence and presence of in the chloramphenicol (or other additions when indicated). 1 mL *Synechosystis* cells suspension at 5 μ g Chl/ml was used in each measurement, and three replicates were measured.

3.1.3. Photoinhibitory treatment of *Synechocystis* cells

Before starting highlight treatment, cells were left for one hour under growth light 40 μ mol photons m⁻² s⁻¹ at continuous stirring followed by measurement of control value of oxygen evolution rate, which was used as zero time point for the highlight treatment. For photoinhibitory treatment, cells were illuminated with 500 μ mol photons m⁻² s⁻¹ white light without additions, in the presence of the protein synthesis inhibitor lincomycin (300 or 400 μ g mL⁻¹) or chloramphenicol (200 μ g mL⁻¹). The temperature during illumination was maintained at 30 °C. In experiments with protein synthesis inhibitors, cells were incubated at

growth light for 40 min in the absence of inhibitor followed by additional 20 min incubation in the presence of the inhibitor before measuring the control value of oxygen evolution rate.

3.1.4. Statistical analysis

Statistical analysis was performed by one way ANOVA using the Tukey test for means comparison. The calculations were done by the Origin 2018 graphics software. The rates of PSII activity loss obtained from oxygen evolution due to photodamage were calculated by fitting the activity curves with a single exponential decay function $A_i e^{-kt}$, where A_i is the initial activity, k is the rate of activity loss, and t is time).

3.2. Thylakoid and PSII membrane preparation

Thylakoid membranes were isolated from fresh spinach leaves as described earlier by (Berthold et al., 1981), and suspended in a buffer solution containing 50 mM tricine (p^H 7.5), 7 mM $MgCl_2$, 7 mM $CaCl_2$ and 0.3 M Sorbitol. Photosystem II (PSII) membrane particles were isolated from fresh spinach leaves as described earlier by Berthold et al. 1981; Vass et al. 1987, and suspended in a buffer solution containing 40 mM MES-NaOH (pH 6.5), 15 mM $MgCl_2$, 15 mM $CaCl_2$ and 1 M betaine. The BBY membranes were stored in -80 °C for further experiments.

3.2.1. Light-induced oxygen uptake measurement in thylakoid membranes and PSII particles

Steady-state oxygen uptake rates in thylakoid membranes and PSII particles were measured by using a Hansatech DW₂ O₂ electrode (Hansatech instruments Ltd, England) at 4 °C under illumination with 2300 $\mu\text{mole m}^{-2}\text{s}^{-1}$ light intensity. Continuous stirring of the sample was applied during the measurements. The total duration of illumination was 1 min. When indicated 200 $\mu\text{g mL}^{-1}$ chloramphenicol alone or in combination with 20 units/mg superoxide dismutase (SOD) was also present during the measurements. 1 mL aliquot of thylakoid membranes at 25 $\mu\text{g Chl mL}^{-1}$ was used in each measurement, and three replicates were measured. One mL aliquot of PSII membrane particles at concentration 5 $\mu\text{g Chl mL}^{-1}$ was used in each measurement.

3.2.2. Photoinhibitory treatment of thylakoid and PSII membranes

40 mL thylakoid suspension at a concentration of 25 $\mu\text{g Chl/mL}$ was illuminated at of 500 $\mu\text{mole m}^{-2} \text{s}^{-1}$ light intensity with and without chloramphenicol of the indicated concentration. The temperature during illumination was maintained at 4 °C. When indicated the light treatment was performed in the presence of chloramphenicol at (200 $\mu\text{g/mL}$) and superoxide dismutase (20 units/mg). Oxygen evolution of the thylakoid membranes was

measured in 1 mL aliquot using a DW₂ oxygen electrode (Hansatech) at 4 °C under the illumination of 2300 μmol m⁻²s⁻¹ visible light intensity in the presence of artificial electron acceptors 0.5 mM DMBQ at different illumination time points (0, 15, 30, 45) . The PSII particles were resuspended at 5 μg Chl mL⁻¹ in 40 mL volume and illuminated with 500 μmol m⁻²s⁻¹ light intensity in the presence and absence of CAP (200 μg mL⁻¹). The temperature during illumination was maintained at 4 °C. When indicated SOD (20 units mg⁻¹) and/or catalase (1000 unit) was also added. Photosynthetic activity of irradiated PSII membranes was also assessed by measuring the so-called OJIP transient of variable Chl fluorescence during application of a 2 s saturating pulse (Strasser et al., 1995) by using an FL-3000 fluorometer (PSI). F_v/F_m was obtained by calculating (F_m-F_o)/F_m, where F_o and F_m represent the minimum fluorescence in the dark-adapted sample, and the maximal fluorescence yield under saturating light, respectively.

3.3. Thermoluminescence measurements procedure

Flash induced thermoluminescence (TL) measurements were performed as described in (Cser and Vass 2007). Cells equivalent to 30 μg of Chl were pre-illuminated for 30 s with white light at room temperature and then dark-adapted for 3 min at room temperature. Samples without addition were illuminated with a single turnover saturating flash given at +10 °C with or without an additional far-red (FR: 740 nm) illumination, provided by an LED source during cooling of the samples from 0 to -40 °C, or from -10 to -40 °C as indicated in the figures. To block the electron transport at the Q_B site of PSII, 10 μM DCMU was added in the dark and incubated for 3 min followed by FR illumination from -10 ° to -40 °C. After cooling the samples to -40 °C they were heated to 80 °C at a rate of 20 °C min⁻¹ and the luminescence intensity was recorded as a function of temperature. Resolution of the complex TL curves to individual components was performed by a curve fitting method (Vass et al., 1981) using the formula

$$I = AT \exp [(-E/kT) + \frac{S_0}{BE} kT^3 \exp(-E/kT)]$$

(where A is a proportionality factor, E activation energy, B Boltzmann's constant, B heating rate and S₀ frequency factor) for the temperature dependence of the TL intensity. The curve fitting procedure was performed by a Matlab-based software, written by László Sass.

3.3.1 Measurement of chlorophyll fluorescence induction transients

Chlorophyll fluorescence was measured with the Dual-PAM-100 chlorophyll fluorometer (Heinz Walz, Effeltrich, Germany) at 30 °C. A slow induction measuring protocol

was launched and the Chl fluorescence signal was recorded for 30 s in dark to establish a baseline, then the actinic red light (635 nm peak intensity) at $\sim 56 \mu\text{mol photons m}^{-2}\text{s}^{-1}$ was turned on to record light-induced Chl fluorescence variation during 180 s, and thereafter the fluorescent signal was recorded during the light-to-dark transition for an additional 75 s, i.e. to a maximum of 255 s.

4. Results and Discussion

4.1. Chloramphenicol mediates an alternative electron transfer pathway in PSII isolated thylakoid membrane particles, which results in superoxide production and superoxide-induced photodamage

4.1.1. Production of $\text{O}_2^{\bullet-}$ by chloramphenicol in isolated spinach thylakoid

It has been shown earlier that chloramphenicol acts as an electron acceptor in PSI and transfers electrons to O_2 , which results in $\text{O}_2^{\bullet-}$ production (Okada et al., 1991). Since the conversion of O_2 to $\text{O}_2^{\bullet-}$ decreases the concentration of dissolved O_2 the process of CAP-mediated $\text{O}_2^{\bullet-}$ production can be followed by oxygen uptake measurements. Our data, which were obtained in the absence of additions to the thylakoid membranes show that illumination induces an O_2 uptake, which is partly reversed by the addition of SOD (Fig. 4.1.1). These data can be explained by superoxide production in the illuminated thylakoids, which lack added electron acceptors, and therefore the normal LEF pathway is not working. When the O_2 uptake experiments were performed in the presence of lincomycin (+/- SOD) the same results were obtained as in the absence of lincomycin, which show that lincomycin does not interfere with $\text{O}_2^{\bullet-}$ production. In contrast, the addition of CAP largely enhanced the SOD reversible O_2 uptake (Fig. 4.1.1), which demonstrates that CAP enhances $\text{O}_2^{\bullet-}$ production by delivering electrons from the photosynthetic electron transport chain to molecular O_2 .

The partial effect of SOD in reversing the O_2 uptake is explained by the stoichiometry of the SOD effect, which results in the formation of $\frac{1}{2} \text{O}_2$ from 1 $\text{O}_2^{\bullet-}$ (eqn. 1). Therefore, maximum half of the O_2 uptake can be reversed by SOD addition. The reason for the less than 50% reversal of O_2 uptake by SOD shows the presence of other O_2 consuming processes, such as $^1\text{O}_2$ production which results in O_2 uptake due to oxidation of protein/lipid/pigment components, which is not reversible by SOD.

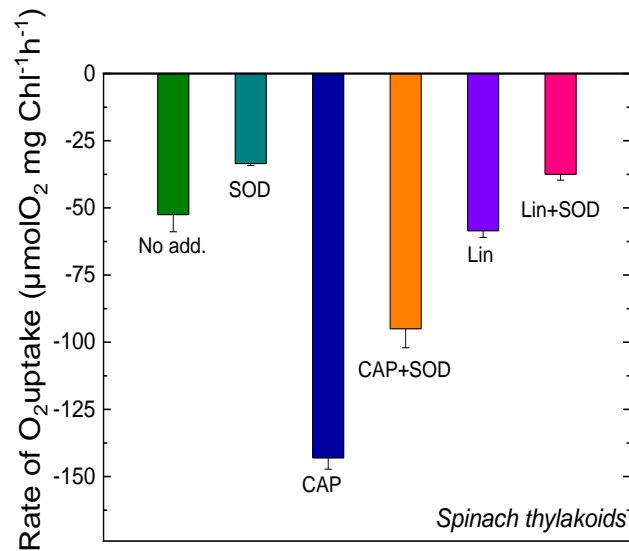


Figure 4.1.1. The effect of chloramphenicol and SOD on the rate of oxygen uptake in spinach thylakoid, rate of oxygen uptake in spinach thylakoid membranes with and without chloramphenicol in combination with SOD. Light intensity during the O₂ measurements was 2300 μmol photons m⁻²s⁻¹.

To investigate the effect of chloramphenicol on the sensitivity of PSII to photoinhibition, the thylakoid membranes were exposed to high light in the absence and presence of chloramphenicol. The thylakoid membranes were also exposed to high light in the presence of superoxide dismutase (SOD) in combination with chloramphenicol. The PSII activity was measured during the course illumination by monitoring the oxygen-evolving activity of the thylakoids using 0.5 mM 2,6-dimethyl-p-benzoquinone (DMBQ) as an artificial electron acceptor. The extent of light-induced PSII photodamage in thylakoid membranes was significantly higher in the presence of chloramphenicol (Fig. 4.1.2.). However, the enhanced photodamage was partly reversed when the thylakoid membranes were exposed to high light in presence of SOD in combination with chloramphenicol (Fig. 4.1.2.). The effect of chloramphenicol on PSII photodamage in thylakoid membranes was confirmed by the application of DMBQ as an electron acceptor.

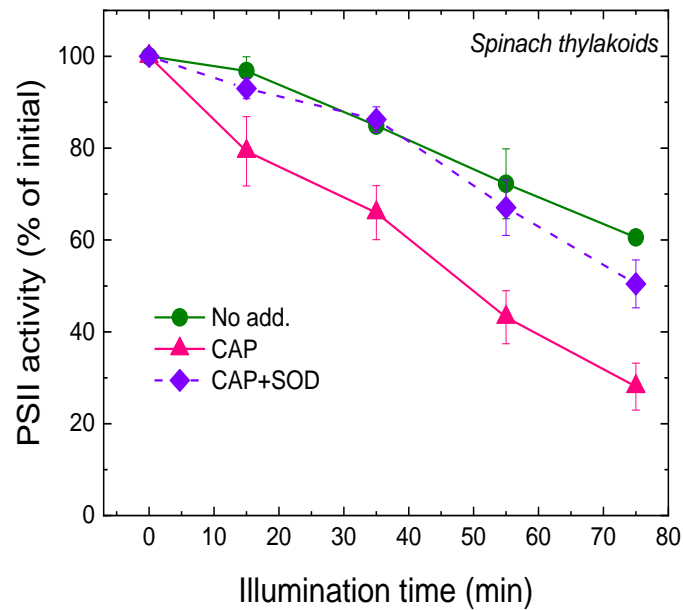


Figure 4.1.2. Effect of chloramphenicol on the extent of light-induced PSII photodamage in spinach thylakoid membranes, In spinach thylakoid membranes, the light induced damage of PSII activity was assessed by measuring the rate of oxygen evolution in the presence of 0.5 mM (DMBQ) as artificial electron acceptor during exposure of thylakoid membranes only (circles), thylakoid membranes with chloramphenicol (triangles) and thylakoid membranes with chloramphenicol+SOD (dash line, squares) to illumination with 500 $\mu\text{mol photons m}^{-2}\text{s}^{-1}$ visible light intensity. Light intensity during the O_2 measurements was 2300 $\mu\text{mol photons m}^{-2}\text{s}^{-1}$.

Photosynthetic activity of irradiated thylakoid membranes without addition, with chloramphenicol and with chloramphenicol+SOD was also assessed by measuring variable chlorophyll fluorescence (Fig. 4.1.3.), F_v/F_m data were obtained by calculating $(F_m - F_0)/F_m$ and the results show light-induced decline of variable chlorophyll fluorescence and F_v/F_m in the presence of chloramphenicol.

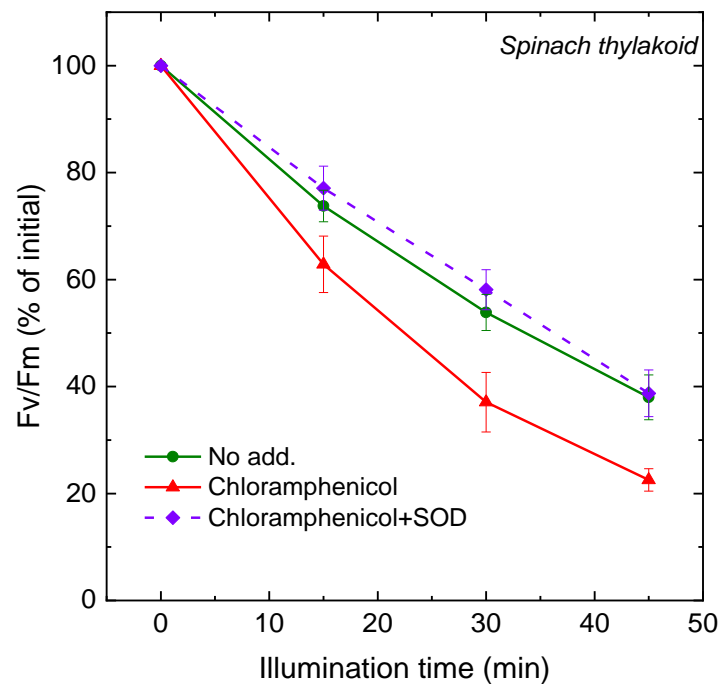


Figure 4.1.3. The effect of chloramphenicol addition on PSII activity in spinach thylakoid membranes as quantified by fast chlorophyll fluorescence rise, changes in the activity of PSII were followed by calculating photochemical efficiency of PSII (F_v/F_m) during exposure of thylakoid membranes only (circles), thylakoid membranes with chloramphenicol (triangles) and thylakoid membranes with chloramphenicol+SOD (dash line; squares) to illumination with $500 \mu\text{mol photons m}^{-2}\text{s}^{-1}$ visible light intensity. The data represent mean values obtained from three independent experiments, with the indicated SE values.

The consistent restoration of PSII activity has been observed when chloramphenicol was used in combination with SOD. The effect of different concentrations of chloramphenicol on the PSII activity in thylakoid was also quantified by measuring the changes in variable fluorescence and F_v/F_m . The results show chloramphenicol-dependent damage of PSII activity in thylakoid membranes.

Taken together, the data indicate light-induced decline of PSII activity in the presence of chloramphenicol as compared to the control. It shows enhancement of direct photodamage

of the Photosystem II complex. The partial protection of PSII activity in the presence of SOD indicates that the chloramphenicol-induced additional photodamage involves superoxide.

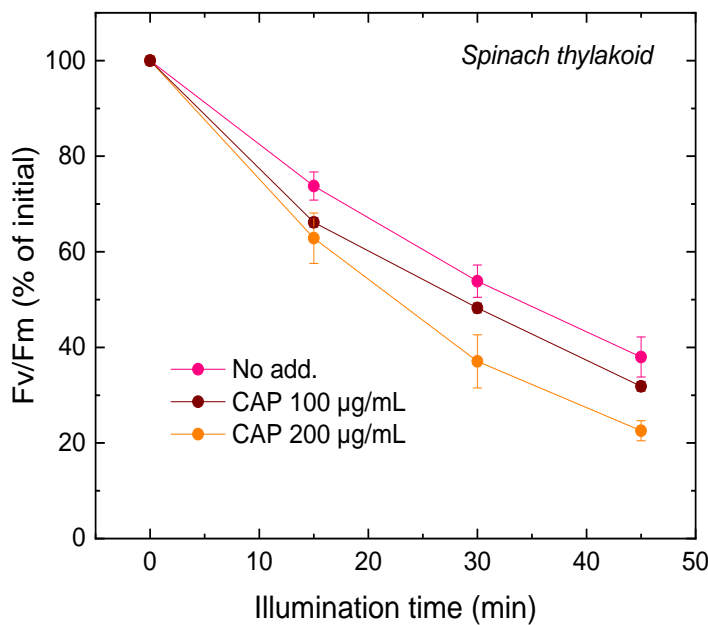


Figure 4.1.4. Concentration dependence of chloramphenicol addition on PSII activity in spinach thylakoid membranes as quantified by changes in variable fluorescence and F_v/F_m . F_v/F_m values calculated during exposure of thylakoid membranes only (circles) or in the presence of 100 $\mu\text{g}/\text{mL}$ (triangles) or 200 $\mu\text{g}/\text{mL}$ chloramphenicol (squares) to illumination with 500 $\mu\text{mol photons m}^{-2}\text{s}^{-1}$ visible light intensity. The data represent mean values obtained from three independent experiments, with the indicated SE values.

In order to quantify the effect of different chloramphenicol concentrations spinach thylakoids were exposed to 500 $\mu\text{mol photons m}^{-2}\text{s}^{-1}$ illumination without addition, and in the presence of 100 μg and 200 $\mu\text{g mL}^{-1}$ CAP as protein synthesis inhibitor. Interestingly, 100 $\mu\text{g mL}^{-1}$ CAP induced only minor enhancement of PSII photodamage relative to that observed in the presence of 200 $\mu\text{g mL}^{-1}$.

4.1.2. Production of superoxide by chloramphenicol in isolated PSII particles

To reveal the effect of chloramphenicol in BBY membrane particles, which contain only PSII, but not PSI complexes, the BBYs membranes were exposed to high light in the presence of CAP and CAP in combination with SOD. The O_2 uptake data show that the

addition of CAP enhances O₂ consumption and this effect is partly reversed by the addition of superoxide dismutase (Fig. 4.1.5.) which suggests that CAP mediated superoxide production occurs in PSII membranes. Importantly, these data demonstrate that chloramphenicol induced superoxide production occurs not only through PSI-mediated electron transport but also in PSII. The O₂ uptake data also show that lincomycin does not induce extra O₂ uptake relative to that of the untreated control.

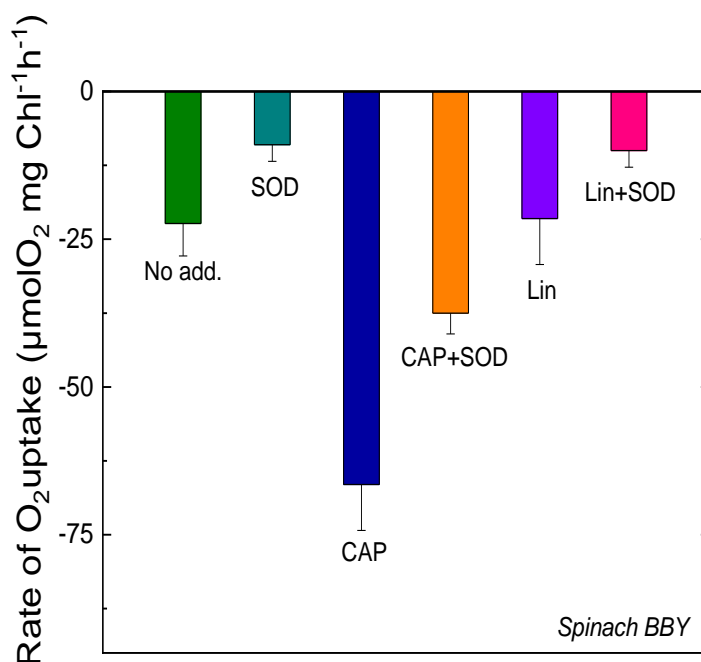


Figure 4.1.5. The effect of chloramphenicol and SOD on the rate of oxygen uptake in spinach BBY particles. Rate of oxygen uptake in BBY membranes with and without CAP in combination with SOD. Light intensity during the O₂ measurements was 2300 µmol photons m⁻² s⁻¹

The effect of CAP on the PSII activity was also assessed by measuring F_v/F_m data (Fig. 4.1.6). The results show the light-induced decline of variable chlorophyll fluorescence (F_v/F_m) in the presence of chloramphenicol. However, the PSII activity has been reversed when SOD was present together with chloramphenicol, which indicates that CAP mediated PSII photodamage proceeds via the production of superoxide.

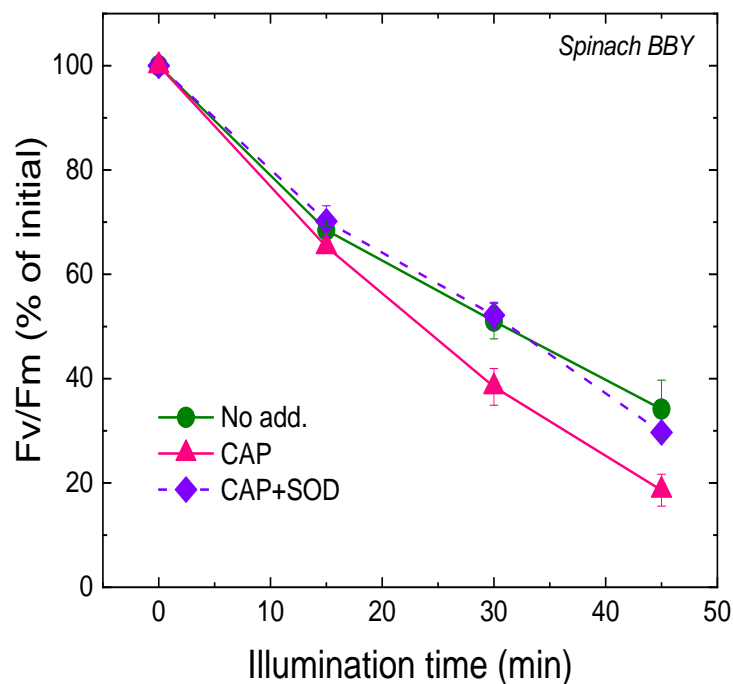


Figure 4.1.6. The effect of chloramphenicol addition on PSII activity in BBY membranes as quantified by fast chlorophyll fluorescence rise, changes in the activity of PSII were followed by calculating photochemical efficiency of PSII (F_v/F_m) during exposure of thylakoid membranes only (circles), thylakoid membranes with CAP (triangles) and thylakoid membranes BBY with CAP+SOD (dash line; squares) to illumination with $500 \mu\text{mol photons m}^{-2} \text{s}^{-1}$ visible light intensity. The data represent mean values obtained from three independent experiments, with the indicated SE values.

4.1.3. Chloramphenicol acts as electron acceptor in PSII

In order to check whether CAP can take electrons directly from PSII the so-called OJIP transient was measured in the presence and absence of CAP in PSII membrane particles, which lack PSI. We observed that the maximal fluorescence F_m was decreased in the presence of CAP, which indicates the presence of electron sink that competes with the accumulation of reduced Q_A .

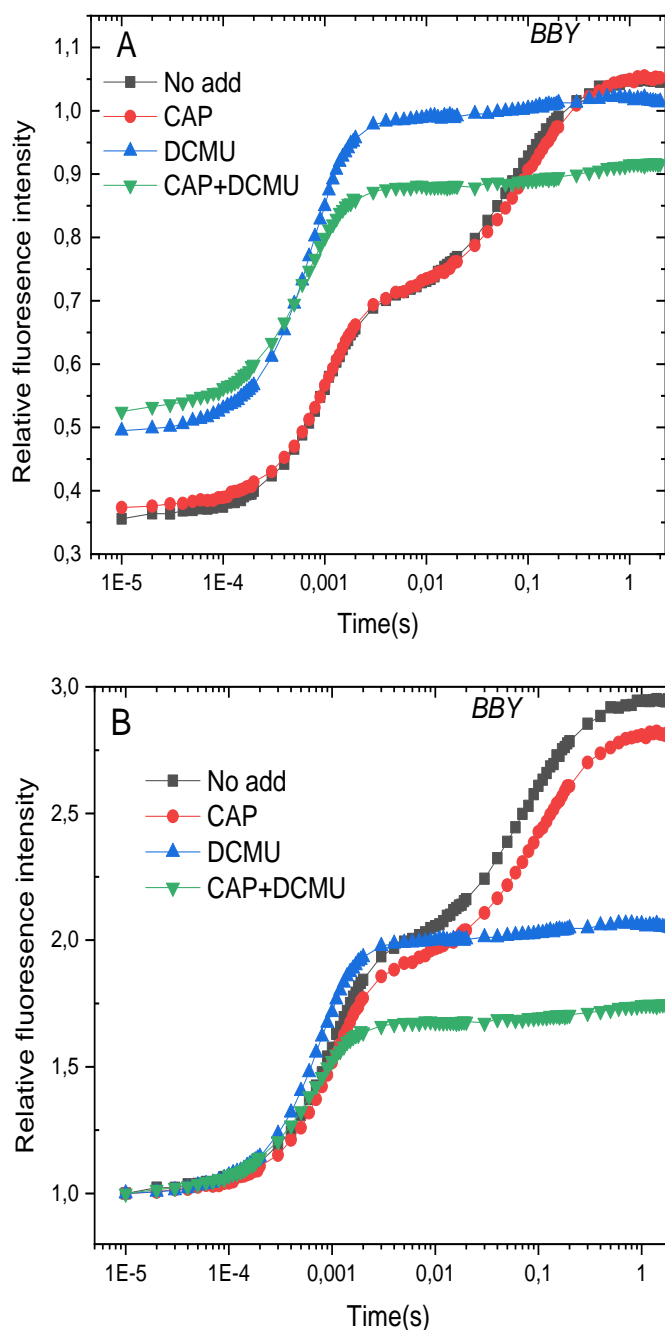


Figure 4.1.7. The effect of CAP on PSII activity in PSII membrane particles as quantified by fast chlorophyll fluorescence rise. Photosynthetic activity of spinach PSII membranes was assessed by measuring OJIP transients of chlorophyll fluorescence. The experiments were performed in the absence (closed symbols) and presence of CAP (open symbols) without further addition (circles) or in the presence of 10 μ M DCMU (triangles). The curves are shown before (A) and after (B) normalization to the same F_0 values.

In Fig. 4.1.7 the fluorescence curves are shown without normalization (A) and after normalization to the F_0 level (B). The addition of electron transport inhibitor DCMU leads to

the back transfer of electrons from Q_A^- to Q_B and therefore F_0 increases. Some decrease in F_m may also occur, which has been attributed to the quenching of fluorescence due to the presence of oxidised PQ pool (Hsu and Lee 1995; Haldimann and Tsimilli-Michael 2005). These two effects lead to the decrease of F_m in the normalized curves, although DCMU does not act as an electron acceptor. The situation is different in the case of CAP, which has only a minor affect on F_0 , but decreases F_m , which is consistent with the presence of an electron acceptor that prevents complete reduction of the Q_A primary quinone electron acceptor. CAP decreases the F_m level also in the presence of DCMU which indicates that CAP takes up electrons from PSII before the DCMU block, i.e., either directly from Q_A^- or from Phe^- .

The redox potential of CAP, $E_m(CAP/CAP^-) = -543$ mV (Kapoor and Varshney 1997), and of $(E_m(Q_A/Q_A^-) = -120$ to -140 mV (Shibamoto et al. 2009). Therefore, the rate of electron transfer from Q_A to CAP should be very low. On the other hand the redox potential of Phe [$E_m(Phe/Phe^-) = -505$ to -535 mV (Shibamoto et al. 2009; Allakhverdiev et al. 2010) allows energetically efficient interaction with Phe^- . Therefore, although the lifetime of Phe^- is very short (ca. 200 ps) it is a possible candidate to act as an electron donor for the reduction of CAP. This finding is in agreement with previous suggestions that Phe^- can act as direct electron donor to O_2 and can support superoxide production (Pospíšil 2012).

4.1.4. Conclusions concerning the effects of CAP on PSII electron transport and photodamage in isolated thylakoids and PSII membrane particles

Our data show that CAP accepts electrons from the PSII complex at a site located before the Q_B quinone electron acceptor, most likely from Phe^- . This process leads to superoxide production, which induces enhanced photodamage of PSII in isolated membrane particles. This side effect of CAP has potentially important implications regarding its application as a protein synthesis inhibitor in photoinhibitory studies. Besides blocking the repair cycle of PSII CAP may accelerate the rate of photodamage also in intact systems leading to artifacts concerning the mechanism of photoinhibition.

4.2. Effect of chloramphenicol on photodamage of intact WT and PSI-less *Synechocystis* cells

4.2.1. Effect of chloramphenicol on the extent of PSII photodamage in WT *Synechocystis* cells

An interesting controversy regarding the side effect of CAP in enhancing the rate of PSII photodamage, concerns the role the OCP protein in photoprotection. It has been reported earlier that the orange carotenoid protein (OCP) has a very efficient $^1\text{O}_2$ scavenging activity and provides protection against $^1\text{O}_2$ -mediated photodamage of PSII in *Synechocystis* cells (Sedoud et al. 2014). However, the hypothesis that OCP would decrease direct damage of by $^1\text{O}_2$ was criticized by (Kusama et al. 2015) claiming that $^1\text{O}_2$ affects only PSII repair, and no enhanced damage can be observed when CAP is used as protein synthesis inhibitor (Kusama et al. 2015). In an attempt to resolve this contradiction Rehman has compared high light-induced PSII activity loss in WT and ΔOCP cells in the presence of lincomycin or CAP (Rehman 2016). These results showed that the OCP mutant cells were photodamaged faster than WT cells in the presence of lincomycin. However, this difference could not be observed when CAP was used as protein synthesis inhibitor, and PSII activity loss showed practically the same time dependence in the WT and ΔOCP cells presence of CAP (Rehman 2016) confirming the findings of (Kusama et al. 2015). These results were interpreted as showing show that CAP accelerated photodamage relative to that observed in the presence lincomycin and this effect masked the difference between the rate of PSII photodamage in the WT and ΔOCP (Rehman 2016). However, this hypothesis was not investigated further in the previous study (Rehman 2016) and no unambiguous proof was provided for its validity. Since it is very important to know if CAP induces an artifact by accelerating PSII damage or not, we aimed to clarify this topic by more detailed investigations.

In order to quantify the effect of $200\ \mu\text{g mL}^{-1}$ CAP on the rate of PSII photodamage, WT *Synechocystis* cells were exposed to $500\ \mu\text{mol photons m}^{-2}\ \text{s}^{-1}$ illumination without addition, and in the presence of either lincomycin or CAP as protein synthesis inhibitor. High light alone induced only a small extent of PSII activity loss, as quantified by the rate of oxygen evolution in the presence of $0.5\ \text{mM}$ DMBQ as an artificial acceptor. After 70 min illumination, PSII activity declined to 90% of its initial value (Fig. 4.2.1, squares). In the presence of lincomycin, PSII inactivation was enhanced and the residual activity declined to 55% of its initial value after 70 min (Fig. 4.2.1, circles).

When $200 \mu\text{g mL}^{-1}$ CAP was used as a protein synthesis inhibitor instead of lincomycin, the extent of PSII deactivation was further enhanced, and the residual activity after 70 min illumination was only ca. 40% of its initial value (Fig. 4.2.1., down triangles). The lower part of Fig. 4.2.1. shows that the differences in PSII activity values were statistically significant at each time point for the no addition vs. lincomycin, no addition vs. CAP, and lincomycin vs. CAP treatments at $p < 0.01$ (or 0.001) significance level. In order to make sure that the enhanced loss of PSII activity in the presence of CAP was a real effect and not caused by partial inhibition of protein synthesis in the presence of the applied $300 \mu\text{g mL}^{-1}$ concentration of lincomycin, the photoinhibitory experiments were also performed in the presence of $400 \mu\text{g mL}^{-1}$ lincomycin. These data confirmed that lincomycin at $300 \mu\text{g mL}^{-1}$ concentration was sufficient for full inhibition of protein synthesis (Fig. 4.2.2.).

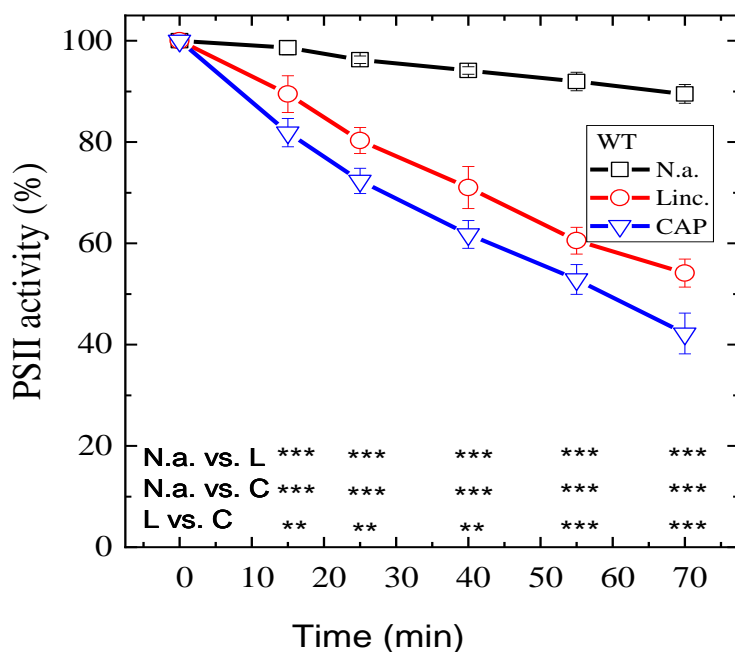


Figure 4.2.1. Impact of chloramphenicol on the extent of light-induced PSII photodamage in *Synechocystis A*, The light-induced damage of PSII activity was evaluated by measuring the rate of oxygen evolution in the presence of 0.5 mM (DMBQ) as artificial electron acceptor during exposure of cells left untreated (squares), treated with $300 \mu\text{g mL}^{-1}$ lincomycin (circles), or $200 \mu\text{g mL}^{-1}$ CAP (down triangles) to illumination with $500 \mu\text{mol photons m}^{-2} \text{ s}^{-1}$ visible light intensity.

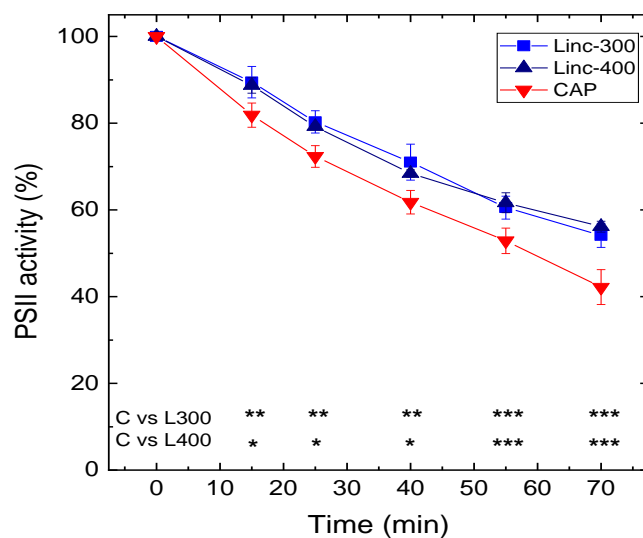


Figure 4.2.2. Effect of concentration of lincomycin on the rate of photodamage using $300 \mu\text{g mL}^{-1}$ lincomycin (triangles), $400 \mu\text{g mL}^{-1}$ lincomycin (squares) in WT *Synechocystis* cells. Light intensity during the O_2 measurements was $2300 \mu\text{mol photons m}^{-2} \text{s}^{-1}$. The asterisk signs indicate the time points where the PSII activity values are significant (* $p < 0.05$, ** $p < 0.01$, *** $p < 0.001$) different between the untreated (n.a.), lincomycin (L) or CAP (C) treated. The percentage of the initial PSII activity, which was obtained from the growth-light-adapted cultures prior to the commencement of high light illumination the differences in PSII activity values were statistically significant at each time point for the no addition vs. lincomycin, no addition vs. CAP, and lincomycin vs. CAP treatments.

4.2.2. Effect of lincomycin and chloramphenicol concentration on PSII photodamage and recovery in WT *Synechocystis*

In the majority of photosynthetic applications CAP is applied in $200 \mu\text{g mL}^{-1}$ or higher concentrations (Briantais et al. 1988; Kettunen et al. 1991; Franklin et al. 1992; Hurry and Huner 1992; Tyystjärvi et al. 1992; Osmond et al. 1993; Stapel et al. 1993; Havaux 1994; Gong 1994; Vavilin et al. 1995; Trebst and Soll-Bracht 1996; Zhang et al. 1997, 2011, 2015; Gombos et al. 1997; Da Matta and Maestri 1998; Depka et al. 1998; Jahns et al. 2000; Apostol et al. 2001; Rodrigues et al. 2002; Alfonso et al. 2004; Nishiyama et al. 2004; Takahashi et al. 2010, 2013; Inoue et al. 2011; Chen et al. 2011; Bhagooli 2013; Jimbo et al. 2013; Kusama et al. 2015; Nagao et al. 2016; Sae-Tang et al. 2016; Ueno et al. 2016). However, in some studies $100 \mu\text{g mL}^{-1}$ or even as low as $30\text{--}50 \mu\text{g mL}^{-1}$ was also used

(Greer et al. 1986; Demmig-Adams and Adams 1993; Vonshak et al. 1994; Mart et al. 1997; Komenda 1998; Komenda and Masojídek 1998; Komenda et al. 1999; Saradhi et al. 2000; Stamenković and Hanelt 2013). Therefore, we aimed to check if these lower concentrations also enhance PSII photodamage. Our data show that PSII activity loss in the presence of $100 \mu\text{g mL}^{-1}$ CAP was practically identical with that observed in the presence of $300 \mu\text{g mL}^{-1}$ lincomycin Fig. 4.2.3. In contrast, $50 \mu\text{g mL}^{-1}$ CAP resulted in a slower loss of PSII activity than lincomycin. In addition, some recovery was also observed under low light conditions following the photoinhibitory treatment, which indicates that $50 \mu\text{g mL}^{-1}$ CAP is not sufficient for complete blocking of PSII repair under our experimental conditions.

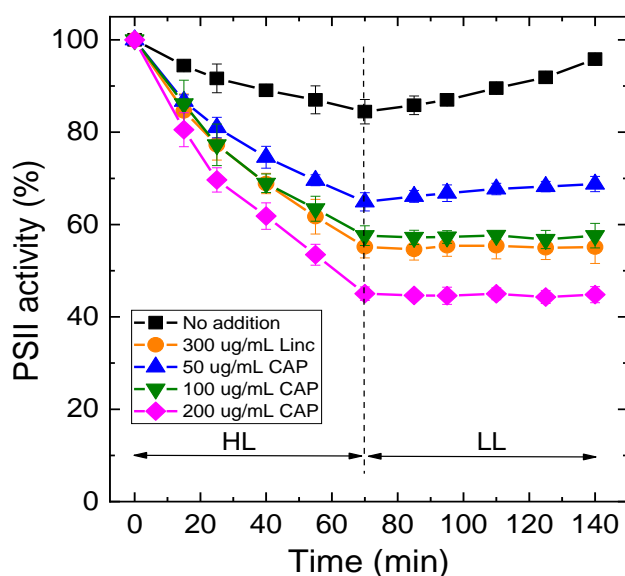


Figure 4.2.3. Effect of lincomycin and chloramphenicol concentration on PSII photodamage and recovery. WT *Synechocystis* cultures were subjected to $500 \mu\text{mol photons m}^{-2}\text{s}^{-1}$ intensity illumination. The cultures were either without the addition of protein synthesis inhibitor (squares), or were treated with lincomycin ($300 \mu\text{g mL}^{-1}$, circles, respectively), and with CAP (50 , 100 , and $200 \mu\text{g mL}^{-1}$, shown by up triangles, down triangles, and lozenges, respectively). PSII activity was estimated by measuring the rate of oxygen evolution in the presence of 0.5 mM DMBQ as an artificial acceptor. The data represent the average of 4 to 6 biological replicates with the standard errors given, and expressed as percentage of the initial PSII activity, which was obtained from the growth-light-adapted cultures before the commencement of high light illumination

The rates of PSII activity loss were calculated by fitting the activity curves with a single exponential decay function. The calculated rates of WT are summarized in Table 1, which shows that the $k = 0.0016 \text{ min}^{-1}$ rate of photodamage, which was observed in the absence protein synthesis inhibitors was increased to 0.0090 min^{-1} in the presence of $400 \mu\text{g mL}^{-1}$ lincomycin. Practically the same photodamage rate (0.0083 min^{-1}) was obtained in the presence of $100 \mu\text{g mL}^{-1}$ CAP. However, the damage rate was increased by ca. 50% (to 0.0120 min^{-1}) when $200 \mu\text{g mL}^{-1}$ CAP was applied showing a concentration dependence of CAP-induced photodamage. The calculated rates of glucose grown WT which shows the rate of photodamage in the absence of protein synthesis inhibitor $K=0.0015 \text{ min}^{-1}$ and in the presence of applied protein synthesis inhibitor $300 \mu\text{g mL}^{-1}$ lincomycin $K=0.0085 \text{ min}^{-1}$ and when $200 \mu\text{g mL}^{-1}$ CAP was applied the rate of photodamage was increased to 0.0119 min^{-1} . The calculated rates of glucose grown PSI-less which shows the rate of photodamage in the absence of protein synthesis inhibitor $K=0.0035 \text{ min}^{-1}$ and in the presence of applied protein synthesis inhibitor $300 \mu\text{g mL}^{-1}$ lincomycin $K=0.0152 \text{ min}^{-1}$ and when $200 \mu\text{g mL}^{-1}$ CAP was applied the rate of photodamage was increased to 0.0217 min^{-1} of ca. 20%.

Table 1. Rates of PSII photodamage

Sample	Rate of photodamage (min^{-1})	
	Mean	Stdev
WT	0.0016	1.42E-04
WT+300 linc	0.0088	3.13E-04
WT+400 linc	0.0090	9.77E-04
WT+100 CAP	0.0083	1.24E-03
WT+200 CAP	0.0120	6.59E-04
WT+gluc	0.0015	1.36E-04
WT+gluc+300 linc	0.0085	3.65E-04
WT+gluc+200 CAP	0.0119	8.23E-04
PSI-less+gluc	0.0035	5.41E-04
PSI-less+gluc+300 linc	0.0152	5.51E-04
PSI-less+gluc+200 CAP	0.0217	1.23E-03

Synechocystis cultures were exposed to $500 \mu\text{mol m}^{-2}\text{s}^{-1}$ light and their photosynthetic activity was followed as a function of illumination time by measuring the rate of oxygen evolution in the presence of DMBQ as artificial acceptor. PSII photodamage rates were calculated by fitting the activity curves with a single exponential decay function ($A_i e^{-kt}$, where A_i is the initial activity, k is the photodamage rate, and t is time). The experiments were performed in photoautotrophically grown WT cells, without addition, and in the presence of protein synthesis inhibitors (300 and $400 \mu\text{g mL}^{-1}$ lincomycin, $200 \mu\text{g mL}^{-1}$ CAP, abbreviated as CAP). The photoinhibitory treatments were also performed in a PSI-less *Synechocystis* mutant line, which cannot grow photoautotrophically, and therefore was cultured photomixotrophically in the presence of 5 mM glucose (PSI-less+gluc). As a control for the PSI-less mutant, the WT cells were also grown photomixotrophically (WT+gluc). The PSI-less+gluc and WT+gluc cultures were exposed to the same high light and inhibitor treatments as the photoautotrophically grown WT.

4.2.3. Chloramphenicol enhances PSII photodamage in comparison to lincomycin in PSI-less *Synechocystis*

In order to clarify if the photodamage-enhancing effect of CAP is related to its interaction with PSI or PSII, the light treatment experiments were also performed in a *Synechocystis* mutant, which lacks PSI. In contrast to the WT strain, high light exposure alone induced a substantial loss of PSII activity in the PSI-less mutant, which resulted in a decline to ca. 77% of the initial activity after a 70 min illumination (Fig. 4.2.4, squares). The addition of lincomycin enhanced the activity loss to ca. 35% of the initial activity after a 70-min illumination (Fig. 4.2.4 circles). In the presence of $200 \mu\text{g mL}^{-1}$ CAP the extent of PSII deactivation was further enhanced, leading to residual activity of ca. 20% of the initial activity after 70 min (Fig. 4.2.4, down triangles). The lower part of the figure shows that the differences in PSII activity values were statistically significant in each time point for the no addition vs. lincomycin, no addition vs. CAP, and lincomycin vs. CAP treatments at $p < 0.05$ (0.01, or 0.001) significance level (see also Table 1). The calculated rates of PSII photodamage confirm that $200 \mu\text{g mL}^{-1}$ CAP enhances photodamage also in the PSI-less mutant ($k = 0.0217 \text{ min}^{-1}$) relative to that observed in the presence of lincomycin ($k = 0.0152 \text{ min}^{-1}$).

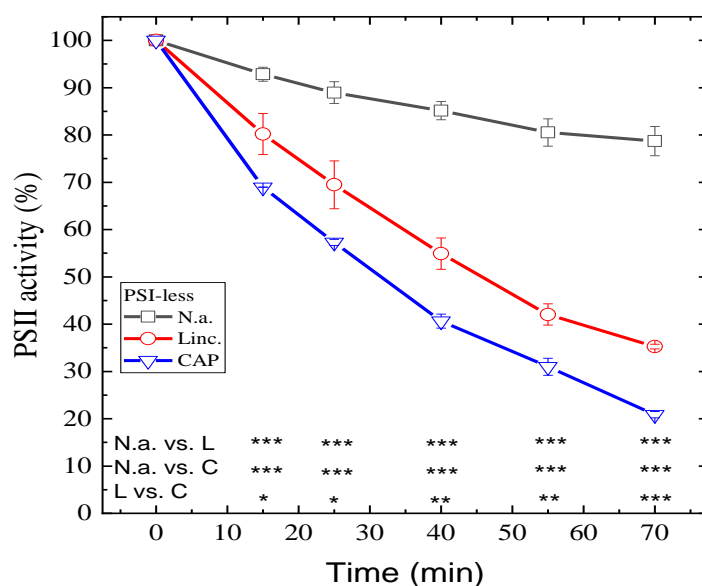


Figure 4.2.4. Differential effects of lincomycin and chloramphenicol on photoinhibitory activity loss in PSI-less *Synechocystis* cells. PSI-less *Synechocystis* cultures were exposed to $500 \mu\text{mol photons m}^{-2} \text{s}^{-1}$ intensity illumination. The cultures were left untreated (squares), treated with $300 \mu\text{g mL}^{-1}$ lincomycin (circles), or $200 \mu\text{g mL}^{-1}$ CAP (down triangles). PSII activity was evaluated by measuring the rate of oxygen evolution in the presence of 0.5 mM DMBQ as an artificial acceptor. Data are shown as a percentage of the initial PSII activity, which was obtained from the growth-light-adapted cultures before the initiation of high light illumination. The asterisk signs indicate the time points at which PSII activity values are significant (* $p < 0.05$, ** $p < 0.01$, *** $p < 0.001$) different between the non-treated (n.a.), lincomycin (L) or CAP (C) treated samples

4.2.4. Effect of photoheterotrophic growth on photoinhibitory activity loss in WT *Synechocystis* cells

The light-induced loss of PSII activity is apparently enhanced in the PSI-less mutant when compared to the WT (Fig. 4.2.1. vs. Fig. 4.2.4). However, we have to note that the growth conditions for the WT and the PSI-less strain were different (photoautotrophic growth at $40 \mu\text{mol photons m}^{-2} \text{s}^{-1}$ for the WT, and photomixotrophic growth in the presence of 5 mM glucose at $4 \mu\text{mol photons m}^{-2} \text{s}^{-1}$ for the PSI-less mutant). In order to clarify if the enhanced photodamage of PSII activity is due to the lack of PSI, or occurs as a consequence of different growth conditions, the light treatments were also performed in WT cells that were grown under the same conditions as the PSI-less mutant. Growing the WT cells in the presence of glucose and low light did not affect their light sensitivity when compared to those

grown photoautotrophically at standard light intensity (Fig. 4.2.5). However, pairwise comparison of the activity loss curves in cells which were cultured under the same conditions (photomixotrophy and low light) reveal that PSII photodamage is significantly larger in the PSI-less strain than in the WT. This effect was observed in all three treatment conditions, i.e., without addition, in the presence of lincomycin, or in the presence of CAP (Fig. 4.2.5). The calculated rates of PSII photodamage are also ca. twofold higher in the PSI-less mutant than in the WT grown under photoautotrophic and mixotrophic condition (Table 1).

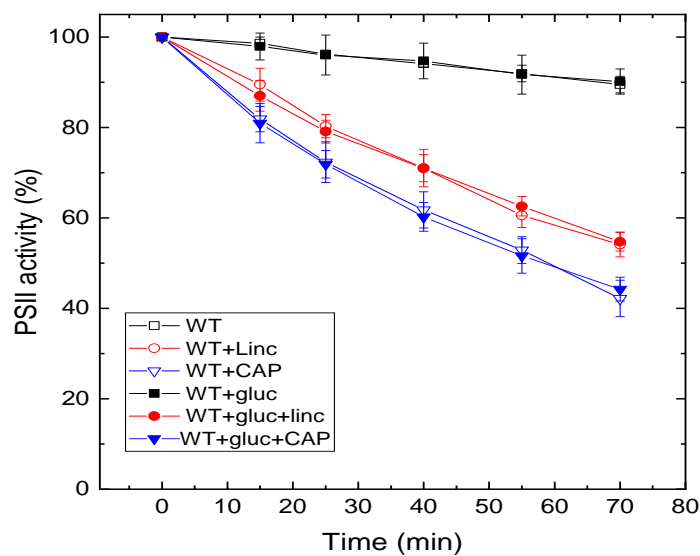


Figure 4.2.5. Effect of glucose on the photoinhibitory effect on WT *Synechocystis* cultures. Cells were grown either in glucose-free BG 11 medium at $40 \mu\text{mol photons m}^{-2}\text{s}^{-1}$ light intensity (open symbols), or in the presence of 5 mM glucose at $5 \mu\text{mol photons m}^{-2}\text{s}^{-1}$ light intensity (closed symbols). The cultures were left untreated (squares), treated with $300 \mu\text{g mL}^{-1}$ lincomycin (circles) or $200 \mu\text{g mL}^{-1}$ CAP (down triangles) and were exposed to $500 \mu\text{mol photons m}^{-2} \text{s}^{-1}$ intensity illumination. PSII activity was assessed by measuring the rate of oxygen evolution in the presence of 0.5 mM DMBQ as artificial acceptor. Data are shown as percentage of the initial PSII activity, which was obtained from the growth-light-adapted cultures before the onset of high light illumination.

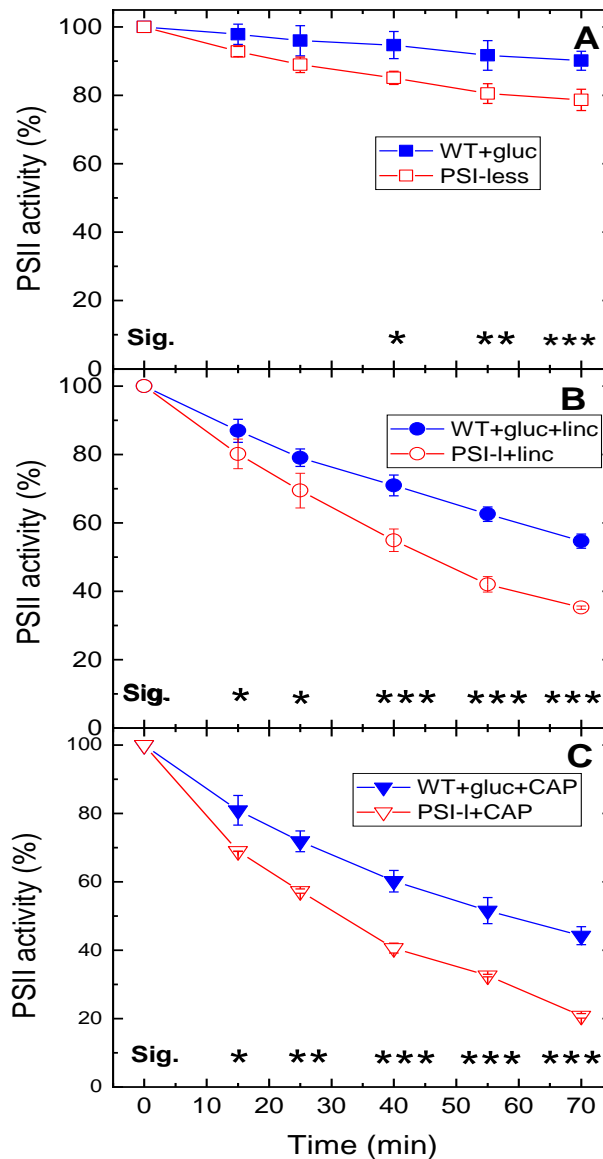


Figure 4.2.6. Differential light sensitivity of WT and PSI-less *Synechocystis* cells. WT (closed symbols) and PSI-less *Synechocystis* cultures (open symbols) were grown in the presence of 5 mM glucose at $5 \mu\text{mol photons m}^{-2} \text{s}^{-1}$ light intensity. The cultures were left untreated (squares), treated with $300 \mu\text{g mL}^{-1}$ lincomycin (circles), or $200 \mu\text{g mL}^{-1}$ CAP (down triangles) and were exposed to $500 \mu\text{mol photons m}^{-2} \text{s}^{-1}$ intensity illumination. PSII activity was assessed by measuring the rate of oxygen evolution in the presence of 0.5 mM DMBQ as artificial acceptor. Data are shown as percentage of the initial PSII activity, which was obtained from the growth-light-adapted cultures before the onset of high light illumination. The asterisk signs indicate the time points where the PSII activity values are significantly ($*p < 0.05$, $**p < 0.01$, $***p < 0.001$) different between the WT and PSI-less samples.

4.2.5. Chloramphenicol induces oxygen uptake in WT and PSI-less *Synechocystis* cells

A significant decrease in the O_2 evolution rate was observed previously in WT *Synechocystis* cells in the presence of CAP (Rehman 2016). The O_2 evolution measurements

were also performed in the presence of DCMU to avoid the artifact that would arise from a direct effect of CAP on the O₂ evolving activity. These data confirmed that the loss of O₂ evolution observed in the presence of CAP shows O₂ consumption, which could be related to O₂^{•-} formation (Rehman 2016). However, the effect of CAP on O₂ uptake has not been checked previously in a PSI-less mutant and therefore these measurements were performed in this Ph.D work. In order to be able to compare the CAP effect in the WT and PSI-less mutant the O₂ uptake measurements in WT cells were repeated in the present study. Our data show that illumination induces an oxygen uptake in the presence of CAP in the WT *Synechocystis* cells (Fig. 4.2.7 A) and its mutant lacking PSI (Fig. 4.2.7 B). The results show a significant reduction in the rate of O₂ evolution when CAP was added to WT *Synechocystis* cells and its PSI-less mutant. The results were confirmed by measuring the O₂ evolution with CAP in the presence of DCMU. In isolated PSII membranes, it was possible to verify by the addition of SOD that CAP-induced O₂ uptake was due to O₂^{•-} formation (Rehman et al., 2016). SOD is a large enzyme (32.5 kDa molecular weight) which does not penetrate through the cell wall of *Synechocystis*; therefore, SOD addition cannot be used to directly verify CAP-induced O₂^{•-} production in intact *Synechocystis* cells. However, based on the analogy with the situation in the isolated PSII particles (Fig.4.1.1), it is highly likely that CAP addition induced O₂^{•-} production also in the intact cells.

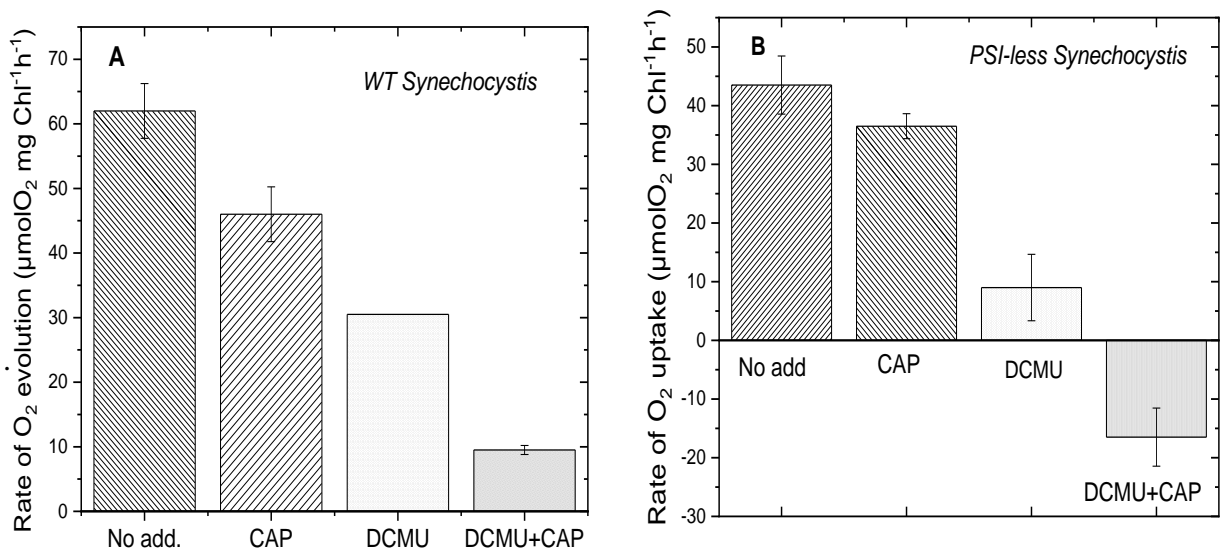


Figure 4.2.7. Effect of CAP on the rate of oxygen evolution in *Synechocystis* cells. A) Rate of oxygen evolution in WT *Synechocystis* cells, with/without DCMU. B) Rate of oxygen evolution in PSI-less *Synechocystis* cells with/without DCMU. Light intensity used during the measurements was 2300 μmol photons m⁻² s⁻¹

4.2.6. Conclusions concerning the effects of chloramphenicol on PSII electron transport and photodamage in intact WT and PSI-less *Synechocystis* cells

4.2.6.1. Chloramphenicol enhances PSII photodamage in intact *Synechocystis* cells

Our data confirm that the rate of photodamage of PSII in intact *Synechocystis* cells is higher in the presence of the usually applied 200 $\mu\text{g mL}^{-1}$ CAP than in the presence of lincomycin (Figs. 4.2.1- 4.2.4). The data presented in Fig. 4.2.2., exclude the possibility that this phenomenon would be caused by a sub-saturating concentration of lincomycin.

The concentration-dependent side effect of CAP was observed in isolated PSII membranes (see above in Chapter 4.1, and in (Rehman et al., 2016)). It was concluded that CAP acts as an electron acceptor in Photosystem II and mediates its superoxide-dependent photodamage in PSII membranes. Since SOD is a large enzyme (32.5 kDa molecular weight), which does not penetrate through the cell wall of *Synechocystis*, SOD addition cannot be used to check the involvement of $\text{O}_2^{\bullet-}$ in CAP induced damage in intact cells. On the other hand, based on the analogy with the results obtained in isolated PSII membrane particles, it is highly likely that $\text{O}_2^{\bullet-}$ production in the presence of CAP is the main cause of enhanced photodamage also in the intact cells.

CAP has been shown to compete with the CO_2 reducing cycle for electrons from PSI because it serves as an electron acceptor of photosystem PSI and its reduction intermediate transfers its electron to molecular oxygen (Okada et.,al 1991). It has also been demonstrated that CAP enhances PSII photodamage via superoxide production in isolated thylakoid preparations (Rehman et al., 2016). Interestingly, the data presented here clearly show that the rate of PSII photodamage is increased practically to the same extent (ca. 37%) both in the WT and the PSI-less strain when CAP is used instead of lincomycin as a protein synthesis inhibitor, which indicates that the damaging mechanism affects primarily PSII.

The CAP-induced enhancement of PSII photodamage is probably related to superoxide production. Therefore, superoxide should be considered as an important reactive oxygen species besides singlet oxygen and hydroxyl radicals, that can damage PSII (Kale et al. 2017; Pospíšil et al. 2019). Superoxide production occurs in PSII during high light exposure, even in the absence of CAP, most likely by reducing oxygen from Phe^- or Q_A^- (Pospíšil 2012).

4.2.6.2. PSII photodamage is enhanced in the absence of PSI

An important finding in our work is that light-induced loss of PSII activity in the presence of protein synthesis inhibitors is much faster in a PSI-less mutant than in the WT

strain containing both PSI and PSII. In the PSI-less mutant the PSI electron pathways, which oxidize the PQ pool, are completely blocked and this results in the reduction of the PQ pool and secondary quinone acceptors, which enhances the production of singlet oxygen acting as a mediator of photodamage (Krieger-Liszkay et al. 2005; Vass and Cser 2009; Vass et al. 2012). Therefore, our data support the idea that enhancement of PSII photodamage in the absence of PSI is related to the lack of efficient electron transport beyond the PQ pool.

4.2.6.3. Chloramphenicol should be used with caution in photoinhibition studies

Our data show that CAP at $200 \mu\text{g mL}^{-1}$, which is a frequently applied concentration in most photosynthesis related studies, enhances photodamage of PSII. Therefore, high CAP amounts should be avoided in studies, which aim at the determination of the true rate of PSII photo-damage. $100 \mu\text{g mL}^{-1}$ CAP appears to be a safe choice since it fully inhibits PSII repair without the side effect of enhanced photodamage rate. It is also of note that the side effect of chloramphenicol (and its recommended safe value) could be influenced by cell density of the culture and the temperature of the photoinhibitory treatment, which are expected to decrease and increase the enhancement of photodamage, respectively

Therefore, it is recommended to check the effect of the applied CAP concentration in comparison with lincomycin when new experimental conditions are designed. The chloramphenicol-induced enhancement of PSII photodamage is probably related to superoxide production. Therefore, superoxide should be considered as an important reactive oxygen species, besides singlet oxygen and hydroxyl radicals, that can damage PSII. The observed enhancement of PSII photodamage in the absence of PSI supports the important role of excitation pressure in influencing the rate of photodamage (Maxwell et al. 1995; Bersanini et al. 2014).

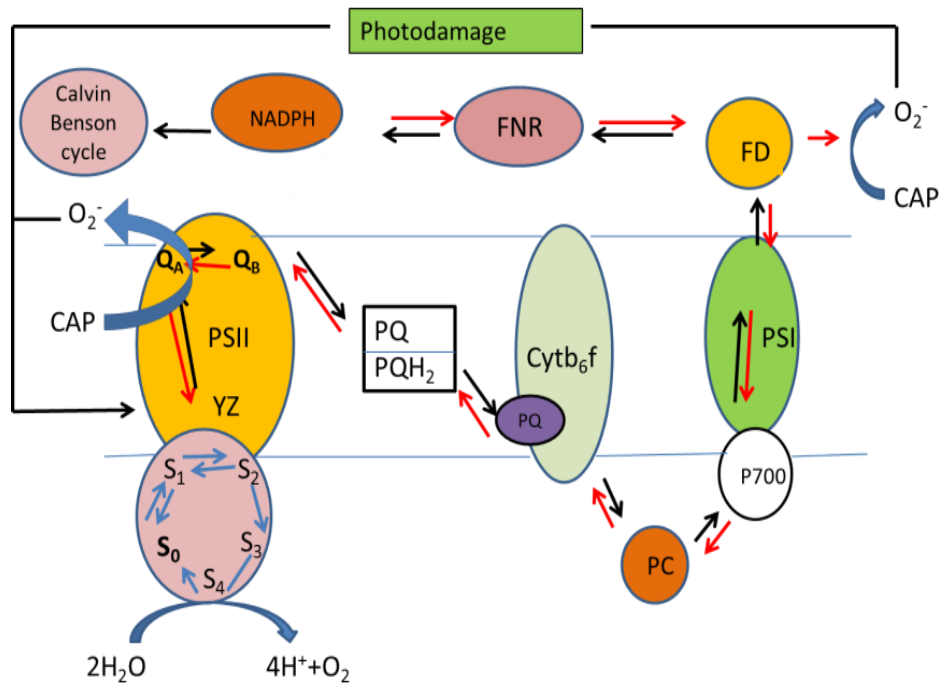


Figure 4.2.8. The proposed mechanism of $O_2^{\bullet -}$ production by chloramphenicol and PSII photodamage; the scheme illustrates the production of superoxide via PSI and PSII by chloramphenicol and in consequence damages PSII.

4.3. Characterization of cyclic electron transport in *Synechocystis* by measuring the AG TL band

The so-called afterglow, AG, thermoluminescence band is a useful indicator of the presence of cyclic electron flow, which is mediated by the NADH dehydrogenase-like (NDH) complex in higher plants. Although NDH-dependent cyclic electron flow occurs also in cyanobacteria, the AG band has previously not been found in these organisms. In order to resolve this contradiction we tested various experimental conditions that could be favorable for the formation of the AG band. One of the conditions was the application of far-red illumination protocols to initiate CEF. Since the abundance of the NDH-1 complex in cyanobacteria depends on the CO_2 level during growth (Battchikova et al. 2011a) we tested both low (air level) CO_2 , which enhances the amount of NDH-1, as well as enhanced CO_2 level, which suppresses the amount of NDH-1.

4.3.1. A +40 °C TL component with AG band characteristics is observed in low CO₂-grown *Synechocystis* cells

When *Synechocystis* cells, grown at ambient CO₂ level, were excited by a single turnover flash from a Xe light source at +10 °C a single TL band was observed at +27 °C which corresponds to the so-called B band (Fig. 4.3.1) originating from the S₂Q_B⁻ charge recombination (Rutherford et al. 1982; Demeter and Vass 1984). However, when cells were excited by continuous FR illumination from -10 to -40 °C a clear shoulder appeared at +40 °C (Fig. 4.3.1)

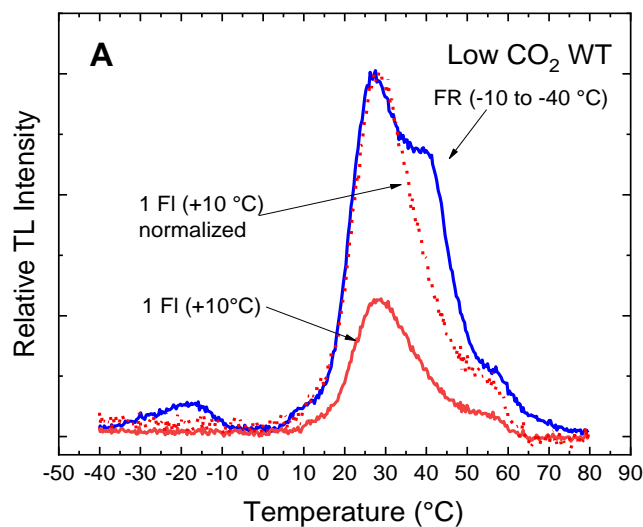


Figure 4.3.1. Thermoluminescence curves of WT *Synechocystis* cells. Low CO₂-grown WT *Synechocystis* cells were illuminated with far-red (FR) light during cooling from -10 to -40 °C (blue curve), with one single turnover flash at +10 °C without FR illumination (solid red curve). The thermoluminescence (TL) curve obtained by the single flash illumination alone is also shown after normalization its amplitude to the maximal intensity of the curve obtained by FR illumination (dotted red).

In order to provide further characterization of +40 °C band we have also checked the effect of FR illumination when it was applied from 0 to -40 °C on the low CO₂ grown cells. This excitation condition generated the B band, but no +40 °C component was observed (Fig. 4.3.2). The FR illumination protocol (from -10 to -40 °C) was also applied in *Synechocystis* cells, which were grown at high CO₂ (3%). Under this condition only the B band, with a slightly downshifted position, was observed together with a small component at +55 °C (Fig. 4.3.2.), which probably represent the so called C-band originating from the Tyr_D⁺Q_A⁻

recombination. The small component at around +5 °C in the high CO₂-grown sample could be partly from the phase transition, and partly of unidentified origin. The small component at around -20 °C, which is observed both in the high and low CO₂-grown samples is possibly related to the A (Tyr_Z⁺Q_A⁻) or ZV (P680⁺Q_A⁻) (Vass et al. 1989) bands.

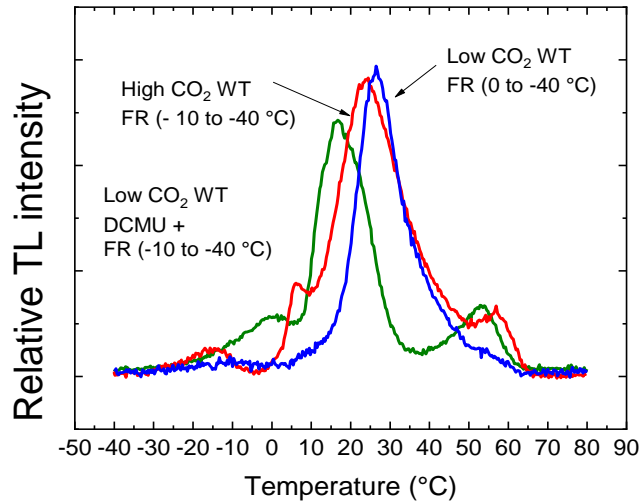


Figure 4.3.2. TL curves were measured after FR illumination of high CO₂-grown WT cells from -10 to -40 °C (red curve), untreated low CO₂-grown cells from 0 to -40 °C (blue curve) or 3,4-dichloro-1,1-dimethyl urea (DCMU) treated low CO₂-grown cells from -10 to -40 °C (green curve).

The FR illumination protocol was also applied to cells, which were treated with DCMU that blocks the Q_B binding site of PSII. Under these conditions the main TL peak appeared at +17 °C (Fig. 4.3.2.), which corresponds to the so-called Q band arising from the S₂Q_A⁻ recombination. The small disturbance of the TL signal at around 0 to +5 °C in the presence of DCMU is the result of a phase transition due to the melting of the sample. Another TL component appeared at +55 °C. This is the so-called C band, arising from the Tyr_D⁺Q_A⁻ recombination. Importantly, no +40 °C TL component was observed in the presence of DCMU, similarly to that reported for the lack of FR-stimulated long-lived AG delayed luminescence in DCMU treated barley protoplasts (Nakamoto et al. 1988).

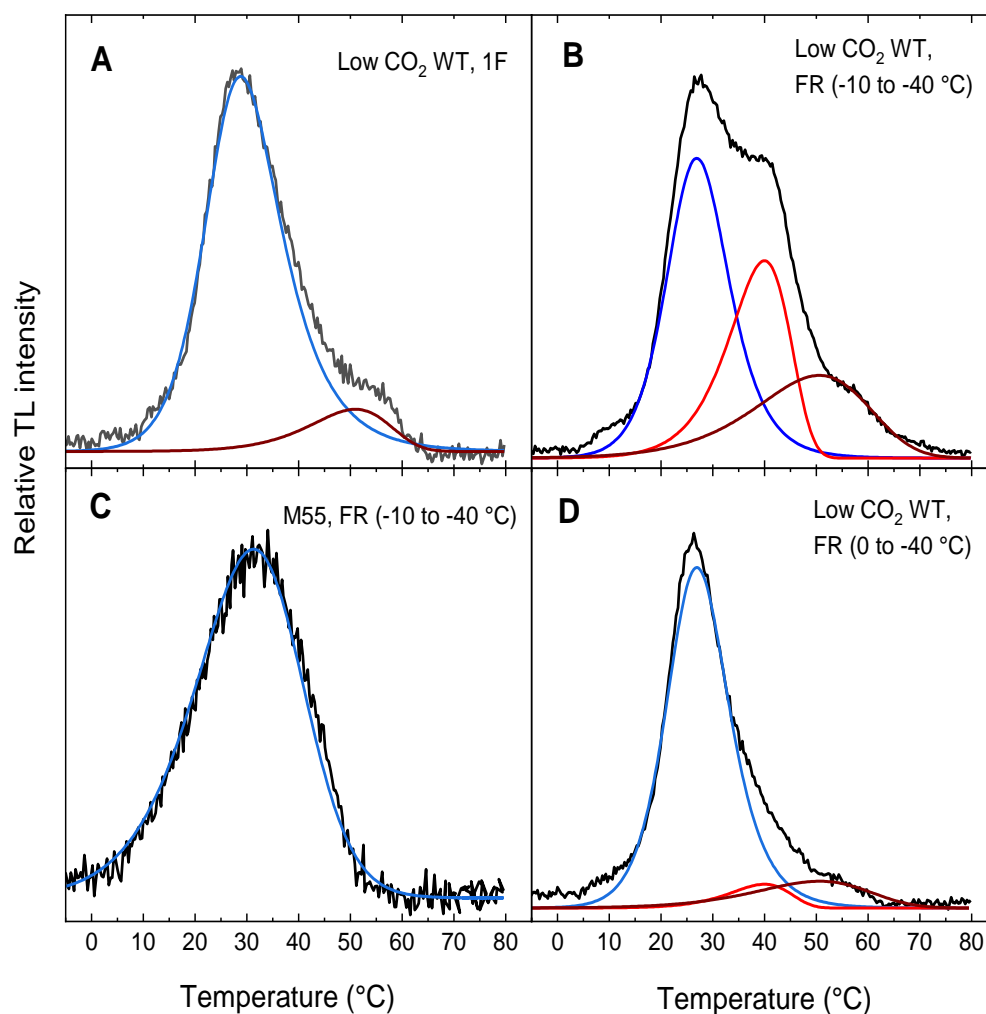


Figure 4.3.3. Identification of individual components in the thermoluminescence (TL) curves of far-red (FR)-illuminated *Synechocystis* cells by curve resolution. TL curves, which were measured as in Figures 4.3.1 and 4.3.2 were resolved to individual components by a curve fitting method.

In order to identify the position of the +40 °C band the measured curves were resolved into individual TL components by using the approach, which was described earlier (Vass et al. 1981) and presented in the Materials and Methods. The results show that the single flash-induced TL band of low CO₂-grown cells is dominated by the B band peaking at +28 °C, with a minor contribution from the C band peaking at +52 °C (Fig. 4.3.3). After illumination with

FR light during cooling from -10 to -40 °C a new TL component appeared at +40 °C besides the main B band and small C band. In the M55 mutant, a single B band was found, peaking at 32 °C (for further discussion see below in chapter 4.3.3.). While illumination of low CO₂-grown WT with FR light from 0 to -40 °C resulted in the B with a very small contribution from the +40 °C and C band

4.3.2. Temperature dependence of the TL curves of far-red light illuminated *Synechocystis* cells

In order to characterize further the peculiar temperature dependence of the AG band generation in *Synechocystis* grown at low CO₂, FR illumination was applied not only during cooling, as in Figures 4.3.1 and 4.3.2, but also at various constant temperatures between +10° and -40 °C. As shown in Figure 4.3.4 FR illumination at +10 °C generated a TL curve, with peak position at around +30 °C, without any clearly resolved +40 °C band. When FR illumination was applied at -10 °C the main peak appeared at +40 °C with a shoulder at around +26 °C, showing that the AG band dominated the FR-induced TL emission under these conditions. When the temperature of the FR illumination was lowered to -20 °C the contribution from the AG was significantly decreased, and was practically absent at -30 and -40 °C FR illumination.

Resolution of the measured TL intensity envelope into components showed a temperature maximum at around -10 °C for the induction of the AG band, and inverse temperature profile for the B band (Fig. 4.3.4B). In higher plants, freezing of leaf samples can decrease or eliminate the AG band due to disruption of the thylakoid and chloroplast structure (Janda et al. 2004). In contrast, *Synechocystis* cells are cooled down to -40 °C before measuring the TL curves without affecting the appearance of the AG and other TL bands. The reason for this difference is most likely the well-known tolerance of cyanobacteria to freezing conditions, which includes their ability to grow in the cryosphere, e.g., in alpine and arctic environment (Vincent 2007), and to survive long-term storage at -80 °C.

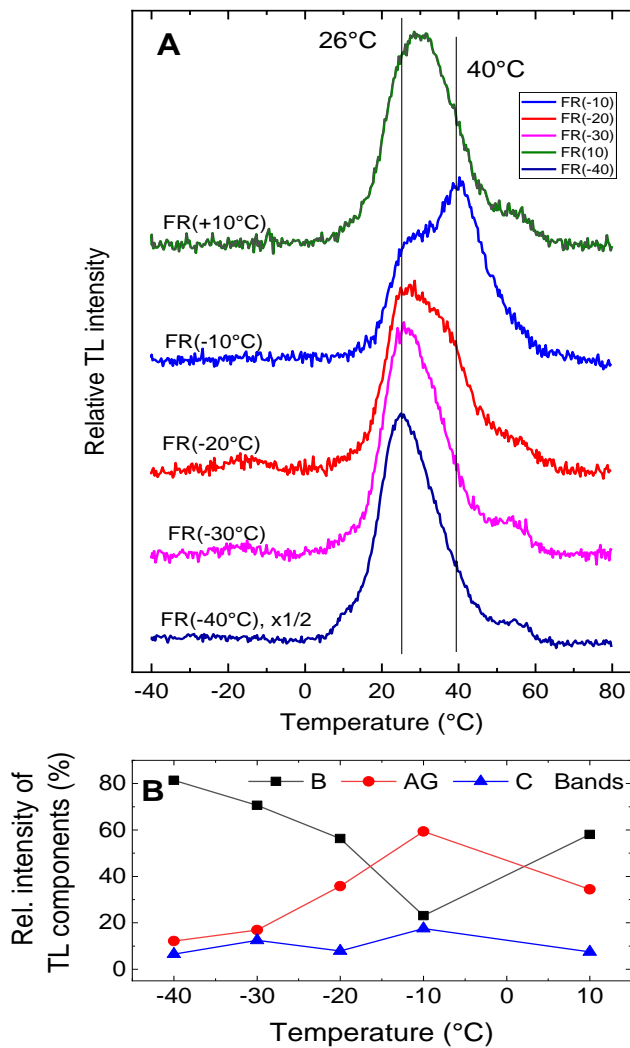


Figure 4.3.4. Temperature dependence of the inducibility of the AG band in *Synechocystis* cells. (A) Thermoluminescence (TL) curves were induced by far-red (FR) light in low CO₂-grown WT *Synechocystis* cells at constant temperatures from +10 to -40 °C as indicated in the curves. (B) The TL curves shown in panel A were deconvoluted into individual components and the relative contribution of the B, AG and C components to the total integrated TL intensity is shown as a function of the temperature where FR illumination was applied.

4.3.3. The 40 °C TL band is missing in the M55 mutant that lacks NDH-1-mediated cyclic electron flow

In plants, the AG band has been assigned to the presence of cyclic electron flow mediated either via the NDH or the PGR-5 pathway (Havaux et al. 2005). In cyanobacteria, the main pathway of cyclic electron flow is mediated by the NDH-1 complex (Battchikova et al. 2011b). In the so-called M55 mutant this pathway is inactivated due to the lack of the *ndhB* subunit (Ogawa 1991). Therefore, we checked the effect of FR illumination in the M55 mutant. As shown in Fig. 4.3.5. continuous illumination during cooling either by white or FR light resulted in essentially the same TL curves showing the main peak at +30 °C, but without any obvious +40 °C component (see also the TL component resolution figure above, Fig.4.3.5, which shows no AG band in the M55 mutant).

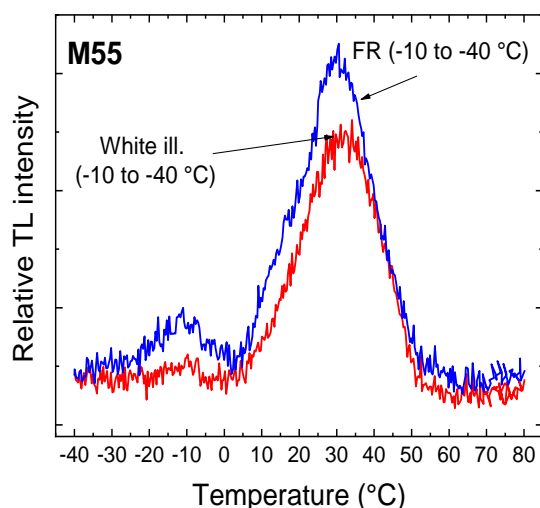


Figure 4.3.5. Thermoluminescence curves of M55 mutant *Synechocystis* cells. Cells were illuminated during cooling from -10° to -40° C either with white light (red curve) or with FR light (blue curve) and TL curves were measured as described in the Materials and Methods.

This finding supports the assignment of the +40 °C band to the NDH1-mediated cyclic electron flow activity. The position of the FR-inducible +40 °C band together with its absence in the M55 mutant and in the presence of DCMU provides further support to the idea that this band is the cyanobacterial counterpart of the AG band that is observed in higher plants and some unicellular algae.

4.3.4. Post-illumination fluorescence rise is connected with the appearance of the +40 °C TL band

Cyclic electron flow returns electrons from the acceptor side of PSI to the PQ pool, which correlates well with the appearance of the so-called post illumination fluorescence rise phenomenon, i.e. the transient rise of the Chl fluorescence yield during the light to dark transition after switching off the actinic light. This phenomenon can be observed both in C4 (Asada et al. 1993), C3 (Mano et al. 1995) plants, and cyanobacteria (Mi et al. 1992) and reflects the CEF via the NDH complex (Mi et al. 1995). The post illumination rise reflects the reduction of the plastoquinone pool via electrons accumulated in the cytosol (Deng et al. 2003). It is a convenient way to study the electron flow around PSI. When we measured the Chl fluorescence yield during dark-light-dark transitions the post illumination rise was present only in the low CO₂-grown WT cells, and it was small in the high CO₂-grown WT and in the *ndhB*-deficient M55 mutant, which is completely devoid of the NDH-1-mediated CEF (Fig. 4.3.6). These findings are consistent with the idea that the NDH-1 complex is produced preferentially under low CO₂ conditions in WT *Synechocystis* cells (Deng et al. 2003) and also that FR-induced CEF is enhanced under these conditions (Deng et al. 2003), which correlates with the appearance of the +40 °C TL band in the low CO₂-grown cells.

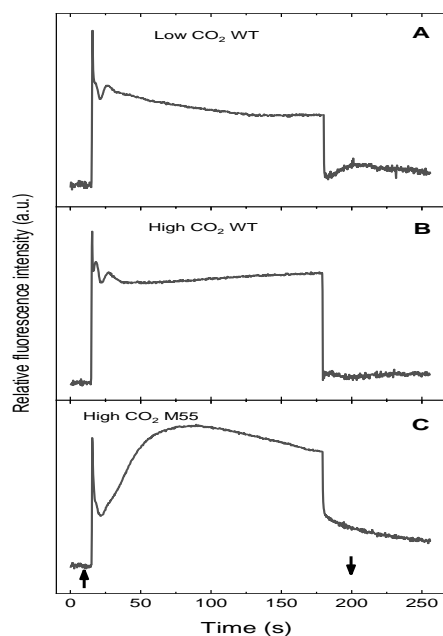


Figure 4.3.6. Variable chlorophyll fluorescence transients of *Synechocystis* cells. Light-induced change in Chl fluorescence was measured by using a DUAL PAM system as described in the Materials and Methods in low CO₂-grown WT (A), high CO₂-grown WT (B), and M55 cells (C).

4.3.5. Conclusions about the origin of the AG band and its connection with NDH-1 mediated CEF

The characteristic temperature dependence of the inducibility of the AG band, with maximal yield at -10 °C, is a very interesting observation, and the most probable reason for that the AG band could not be detected earlier (Havaux et al. 2005). Under normal conditions, illumination produces stable charge separation states in PSII ($S_{2/3}Q_B^-$) in those centers, which were in the $S_{1/2}Q_B$ state prior to the illumination. The recombination of these charge pairs during warming results in the B band. However, in dark-adapted PSII about 50% of the centers has reduced Q_B (i.e., they are in the $S_{1/2}Q_B^-$ state before the illumination (Rutherford et al. 1982; Demeter and Vass 1984). After excitation, these centers will be converted to the $S_{2/3}Q_B$ state, which cannot recombine due to the lack of electrons on Q_B . The AG band is specific in the sense that it arises from those PSII centers in which Q_B is rereduced in the dark via backward electron flow to PQH_2 in the PQ. Cyclic electron flow returns part of the electrons from the acceptor side of PSI, which results in an enhanced reduction of the PQ pool and facilitates the rebinding of PQH_2 , via exchange with the loosely bound Q_B (PQ), to the Q_B site. During this process, the electron can flow backward from Q_B^{2-} to Q_A and Phe via a temperature-activated reverse electron transfer, and can recombine with the $S_{2/3}$ state of the WOC. This process results in the appearance of the AG band of TL. Since the electrons, which participate in the AG band emission, actually originate from PQH_2 they need higher activation free energy for the recombination to produce light-emitting recombination than the electrons, which reside directly on Q_B^- after illumination and participate in the production of the B band. Therefore, the peak temperature of the AG TL band has higher peak temperature (ca. +40 °C) than the B band (26–28 °C). When FR illumination is applied it drives preferentially PSI, and moves electrons from the PQ pool to the acceptor side of PSI. The appearance of both the B and AG bands when samples are illuminated only by FR light is due to the ability of FR illumination to drive electron transfer not only in PSI but also in PSII. The absence of the AG band in the M55 mutant shows that the main pathway responsible for the formation of the AG band involves NDH-1-mediated CEF, similarly to that in higher plants.

In order to observe the AG band in cyanobacteria, the FR illumination should be applied at such temperature, which allows the transfer of electrons from the donor side to the acceptor side of PSI, but does not permit the injection of electrons to the PQ pool via the NDH-1 complex. Our data show that the relative contribution of the AG band to the total TL intensity gradually increases when the temperature of FR illumination is decreased, reaching a maximum at -10 °C (Figure 4.3.4 B). This indicates that the electron transport activity of

NDH-1 becomes inhibited below $-10\text{ }^{\circ}\text{C}$ (Temperature block-1 in Fig. 4.3.7.). Since the contribution of the AG band to the total TL intensity is maximal when FR illumination is applied at $-10\text{ }^{\circ}\text{C}$ (Figure 4.3.4 B), the PSI-mediated electron transfer from the luminal to the stromal side of the thylakoid membrane should be functional at this temperature. Interestingly, a further decrease of the temperature where FR illumination is applied gradually eliminates the AG band (Figure 4.3.4 A, B), which can be explained by assuming a second temperature block in the CEF process either at the donor or acceptor side of PSI.

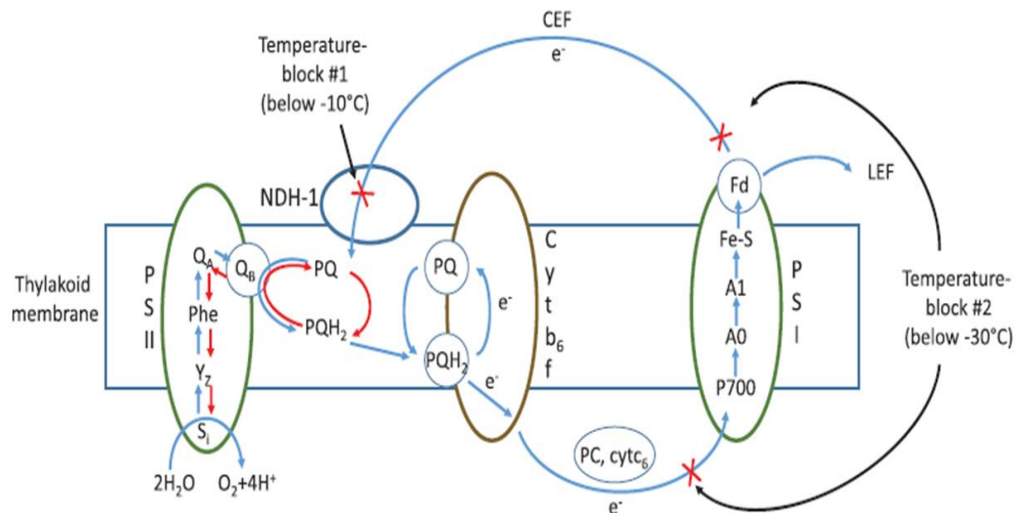


Figure 4.3.7. Scheme of the AG band formation in cyanobacteria. Red arrows show the reversed electron flow, which is initiated by supply of electrons into the PQ pool via NDH-1-mediated CEF, and results in the reduction of Q_B and the consequent charge recombination with the $S_{2/3}$ state leading to the AG TL band emission. The red crosses indicate the putative positions where low temperature induced block of CEF could occur, that can explain the specific temperature dependence of AG band inducibility.

Identification of the AG band in cyanobacteria demonstrates the universal mechanism for the origin of this TL component, and opens the way for its application to study the responses of cyclic electron transport activity under various environmental and stress conditions, including high light. CEF was shown to be upregulated under highlight stress in *Synechocystis* (Thomas et al. 2001). In addition, PSI damage was enhanced in the M55 mutant in absence of NDH-1-mediated photoprotective CEF (Zhao et al. 2018). These findings show that future studies on the characteristics of the AG band have an important potential to obtain a better understanding of the mechanisms of photodamage and photoprotection in cyanobacteria.

5.0. Bibliography

Abasova L, Deák Z, Schwarz R, Vass I (2011) The role of the PsbU subunit in the light sensitivity of PSII in the cyanobacterium *Synechococcus* 7942. *J Photochem Photobiol B Biol* 105:149–156.

Allakhverdiev SI, Tomo T, Shimada Y, et al (2010) Redox potential of pheophytin a in photosystem II of two cyanobacteria having the different special pair chlorophylls. *Proc Natl Acad Sci* 107:3924–3929.

Albertsson P (2001) A quantitative model of the domain structure of the photosynthetic membrane. *Trends Plant Sci* 6:349–358.

Alboresi A, Storti M, Morosinotto T (2019) Balancing protection and efficiency in the regulation of photosynthetic electron transport across plant evolution. *New Phytol* 221:105–109.

Alfonso M, Collados R, Yruela I, Picorel R (2004) Photoinhibition and recovery in a herbicide-resistant mutant from *Glycine max* (L.) Merr. cell cultures deficient in fatty acid unsaturation. *Planta* 219:428–439.

Allahverdiyeva Y, Ermakova M, Eisenhut M, et al (2011) Interplay between flavodiiron proteins and photorespiration in *Synechocystis* sp. PCC 6803. *J Biol Chem* 286:24007–24014.

Allahverdiyeva Y, Mustila H, Ermakova M, et al (2013) Flavodiiron proteins Flv1 and Flv3 enable cyanobacterial growth and photosynthesis under fluctuating light. *Proc Natl Acad Sci USA* 110:4111–4116.

Allakhverdiev SI, Murata N (2004) Environmental stress inhibits the synthesis de novo of proteins involved in the photodamage-repair cycle of Photosystem II in *Synechocystis* sp. PCC 6803. *Biochim Biophys Acta - Bioenerg* 1657:23–32.

Anderson JM, Chow WS (2002) Structural and functional dynamics of plant Photosystem II. *Philos Trans R Soc B Biol Sci* 357:1421–1430.

Apel K, Hirt H (2004) Reactive oxygen species: Metabolism, oxidative stress, and signal transduction. *Annu. Rev. Plant Biol.* 55:373–399

- Apostol S, Briantais J-M, Moise N, et al (2001) Photoinactivation of the photosynthetic electron transport chain by accumulation of over-saturating light pulses given to dark adapted pea leaves. *Photosynth Res* 67:215–227.
- Arntzen CJ, Kyle DJ, Wettren M, Ohad I (1984) Photoinhibition: a consequence of the accelerated breakdown of the apoprotein of the secondary electron acceptor of Photosystem II. *Biosynthesis of the photosynthetic apparatus: Molecular biology, development and regulation* 14:313–324
- Aro E-M, Suorsa M, Rokka A, et al (2005) Dynamics of Photosystem II: a proteomic approach to thylakoid protein complexes. *J Exp Bot* 56:347–356.
- Aro E-M, Virgin I, Andersson B (1993) Photoinhibition of Photosystem II. Inactivation, protein damage and turnover. *Biochim Biophys Acta - Bioenerg* 1143:113–134.
- Aro EM, McCaffery S, Anderson JM (1993b) Photoinhibition and D1 protein degradation in peas acclimated to different growth irradiances. *Plant Physiol* 103:835–843.
- Asada K (1999) THE WATER-WATER CYCLE IN CHLOROPLASTS: Scavenging of active oxygens and dissipation of excess photons. *Annu Rev Plant Physiol Plant Mol Biol* 50:601–639.
- Asada K, Allen J, Foyer CH, Matthijs HCP (2000) The water-water cycle as alternative photon and electron sinks. *Philos Trans R Soc B Biol Sci* 355:1419–1431.
- Asada K, Heber U, Schreiber U (1993) Electron flow to the intersystem chain from stromal components and cyclic electron flow in maize chloroplasts, as detected in intact leaves by monitoring redox change of P₇₀₀ and chlorophyll fluorescence. *Plant Cell Physiol* 34:39–50.
- Barber J, Anderson JM, Telfer A (2002) What is β -carotene doing in the Photosystem II reaction centre? *Philos Trans R Soc London Ser B Biol Sci* 357:1431–1440.
- Barber J, Andersson B (1992) Too much of a good thing: light can be bad for photosynthesis. *Trends Biochem Sci* 17:61–66.
- Barry BA, Babcock GT (1987) Tyrosine radicals are involved in the photosynthetic oxygen-evolving system. *Proc Natl Acad Sci USA* 84:7099–7103.

- Battchikova N, Eisenhut M, Aro EM (2011a) Cyanobacterial NDH-1 complexes: Novel insights and remaining puzzles. *Biochim Biophys Acta - Bioenerg* 1807:935–944.
- Battchikova N, Wei L, Du L, et al (2011b) Identification of novel Ssl0352 protein (NdhS), essential for efficient operation of cyclic electron transport around Photosystem I, in NADPH:plastoquinone oxidoreductase (NDH-1) complexes of *Synechocystis* sp. PCC 6803. *J Biol Chem* 286:36992–37001.
- Berthold DA, Babcock GT, Yocum CF (1981b) A highly resolved, oxygen-evolving Photosystem II preparation from spinach thylakoid membranes: EPR and electron-transport properties. *FEBS Lett* 134:231–234
- Bhagooli R (2013) Inhibition of Calvin–Benson cycle suppresses the repair of Photosystem II in *Symbiodinium*: implications for coral bleaching. *Hydrobiologia* 714:183–190.
- Bialek-Bylka GE, Fujii R, Chen CH, et al (1998) 15-cis-carotenoids found in the reaction center of a green sulfur bacterium *Chlorobium tepidum* and in the Photosystem I reaction center of a cyanobacterium *Synechococcus vulcanus*. *Photosynth Res* 58:135–142.
- Blankenship RE (1992) Origin and early evolution of photosynthesis. *Photosynth Res* 33:91–111
- Blubaugh DJ, Atamian M, Babcock GT, et al (1991) Photoinhibition of hydroxylamine-extracted Photosystem II membranes: identification of the sites of photodamage. *Biochemistry* 30:7586–7597.
- Boyer PD (1997) The ATP synthase—a splendid molecular machine. *Annu Rev Biochem* 66:717–749.
- Briantais J-M, Cornic G, Hodges M (1988) The modification of chlorophyll fluorescence of *Chlamydomonas reinhardtii* by photoinhibition and chloramphenicol addition suggests a form of photosystem II less susceptible to degradation. *FEBS Lett* 236:226–230.
- Bryant DA, Guglielmi G, de Marsac NT, et al (1979) The structure of cyanobacterial phycobilisomes: a model *Arch Microbiol* 123:113–127.
- Burrows PA, Sazanov LA, Svab Z, et al (1998) Identification of a functional respiratory complex in chloroplasts through analysis of tobacco mutants containing disrupted plastid ndh genes. *EMBO J* 17:868–876.

- Campbell DA, Tyystjärvi E (2012) Parameterization of Photosystem II photoinactivation and repair. *Biochim Biophys Acta* 1817:258–265.
- Cape JL, Bowman MK, Kramer DM (2006) Computation of the redox and protonation properties of quinones: Towards the prediction of redox cycling natural products. *Phytochemistry* 67:1781–1788.
- Chen GX, Kazimir J, Cheniae GM (1992) Photoinhibition of hydroxylamine-extracted photosystem II membranes: studies of the mechanism. *Biochemistry* 31:11072–11083.
- Chen YE, Zhang CM, Su YQ, et al (2017) Responses of Photosystem II and antioxidative systems to high light and high temperature co-stress in wheat. *Environ Exp Bot* 135:45–55.
- Chen Z, Lu G, Chen S, Chen X (2011) Light dependency of photosynthetic recovery during wetting and the acclimation of photosynthetic apparatus to light fluctuation in a terrestrial cyanobacterium *Nostoc commune*. *J Phycol* 47:1063–1071.
- Chitnis PR (2001) PHOTOSYSTEM I: Function and Physiology. *Annu Rev Plant Physiol Plant Mol Biol* 52:593–626.
- Chow WS, Aro E-M (2005) Photoinactivation and Mechanisms of Recovery of Photosystem II: The Light-Driven Water: Plastoquinone Oxidoreductase. In: Wydrzynski TJ, Satoh K, Freeman JA (eds). Springer Netherlands, Dordrecht, pp 627–648.
- Cournac L, Guedeney G, Peltier G, Vignais PM (2004) Sustained photoevolution of molecular hydrogen in a mutant of *Synechocystis* sp. strain PCC 6803 deficient in the type I NADPH-dehydrogenase complex. *J Bacteriol* 186:1737–1746.
- Croce R, Van Amerongen H (2014) Natural strategies for photosynthetic light harvesting. *Nat. Chem. Biol.* 10:492–501
- Crofts AR, Meinhardt SW, Jones KR, Snozzi M (1983) The role of the quinone pool in the cyclic electron-transfer chain of *Rhodospseudomonas sphaeroides* A modified Q-cycle mechanism. *BBA - Bioenerg* 723:202–218.
- Cser K, Deák Z, Telfer A, et al (2008) Energetics of Photosystem II charge recombination in *Acaryochloris marina* studied by thermoluminescence and flash-induced chlorophyll fluorescence measurements. *Photosynth Res* 98:131–140.

Cser K, Vass I (2007) Radiative and non-radiative charge recombination pathways in Photosystem II studied by thermoluminescence and chlorophyll fluorescence in the cyanobacterium *Synechocystis* 6803. *Biochim Biophys Acta - Bioenerg* 1767:233–243.

Da Matta FM, Maestri M (1998) Photoinhibition and recovery of photosynthesis in *Coffea arabica* and *C. canephora*. *Photosynthetica* 34:439–446.

DalCorso G, Pesaresi P, Masiero S, et al (2008) A complex containing PGRL1 and PGR5 is involved in the switch between linear and cyclic electron flow in Arabidopsis. *Cell* 132:273–285.

Dall'Osto L, Cazzaniga S, Bressan M, et al (2017) Two mechanisms for dissipation of excess light in monomeric and trimeric light-harvesting complexes. *Nat Plants* 3:17033.

Dartnell LR, Storrie-Lombardi MC, Mullineaux CW, et al (2011) Degradation of cyanobacterial biosignatures by ionizing radiation. *Astrobiology* 11:997–1016.

Davies KM, Anselmi C, Wittig I, et al (2012) Structure of the yeast F1Fo-ATP synthase dimer and its role in shaping the mitochondrial cristae. *Proc Natl Acad Sci USA* 109:13602–13607.

Debus RJ, Barry BA, Sithole I, et al (1988) Directed mutagenesis indicates that the donor to P680⁺ in Photosystem II is tyrosine-161 of the D1 polypeptide. *Biochemistry* 27:9071–9074.

Demeter S, Govindjee (1989) Thermoluminescence in plants. *Physiol Plant* 75:121–130.

Demeter S, Vass I (1984) Charge accumulation and recombination in Photosystem II studied by thermoluminescence. I. Participation of the primary acceptor Q and secondary acceptor B in the generation of thermoluminescence of chloroplasts. *Biochim Biophys Acta - Bioenerg* 764:24–32.

Demmig-Adams B, Adams 3rd WW (1993) The Xanthophyll Cycle, Protein Turnover, and the High Light Tolerance of Sun-Acclimated Leaves. *Plant Physiol* 103:1413–1420.

Demmig B, Winter K, Krüger A, Czygan F-C (1988) Zeaxanthin and the Heat Dissipation of Excess Light Energy in *Nerium oleander* Exposed to a Combination of High Light and Water Stress. *Plant Physiol* 87:17 – 24.

- Demoulin CF, Lara YJ, Cornet L, et al (2019) Cyanobacteria evolution: Insight from the fossil record. *Free Radic Biol Med* 140:206–223.
- Deng Y, Ye J, Mi H (2003) Effects of low CO₂ on NAD(P)H dehydrogenase, a mediator of cyclic electron transport around Photosystem I in the cyanobacterium *Synechocystis* PCC 6803. *Plant Cell Physiol* 44:534–540.
- Deng Y, Ye J, Mi H, Shen Y (2003) Response of NAD(P)H dehydrogenase complex to the alteration of CO₂ concentration in the cyanobacterium *Synechocystis* PCC6803. *J Plant Physiol* 160:967–970.
- Depka B, Jahns P, Trebst A (1998) β -Carotene to zeaxanthin conversion in the rapid turnover of the D1 protein of Photosystem II. *FEBS Lett* 424:267–270.
- Dere S, Gunes T, Sivaci R (1998) Spectrophotometric determination of chlorophyll—A, B and total carotenoid contents of some algae species using different solvents. *TrJ Botany*; 22:13–18
- Ducruet J-M, Roman M, Ortega JM, Janda T (2005) Role of the oxidized secondary acceptor Q_B of Photosystem II in the delayed “afterglow” chlorophyll luminescence. *Photosynth Res* 84:161–166.
- Ducruet JM, Serrano A, Roncel M, Ortega JM (2011) Peculiar properties of chlorophyll thermoluminescence emission of autotrophically or mixotrophically grown *Chlamydomonas reinhardtii*. *J Photochem Photobiol B Biol* 104:301–307.
- Falkowski PG (2006) Tracing Oxygen’s Imprint on Earth’s Metabolic Evolution. *Science* vol 311:1724–1725.
- Fiedor J, Fiedor L, Haeßner R, Scheer H (2005) Cyclic endoperoxides of β -carotene, potential pro-oxidants, as products of chemical quenching of singlet oxygen. *Biochim Biophys Acta - Bioenerg* 1709:1–4.
- Filatov MA, Balushev S, Landfester K (2016) Protection of densely populated excited triplet state ensembles against deactivation by molecular oxygen. *Chem Soc Rev* 45:4668–4689.
- Flint DH, Tuminello JF, Emptage MH (1993) The inactivation of Fe-S cluster containing hydro-lyases by superoxide. *J Biol Chem* 268:22369–22376.

- Formentini L, Sánchez-Aragó M, Sánchez-Cenizo L, Cuezva JM (2012) The mitochondrial ATPase inhibitory factor 1 triggers a ROS-mediated retrograde prosurvival and proliferative response. *Mol Cell* 45:731–742.
- Franklin LA, Levavasseur G, Osmond CB, et al (1992) Two components of onset and recovery during photoinhibition of *Ulva rotundata*. *Planta* 186:399–408.
- Fridovich I (1997) Superoxide Anion Radical (O_2^-) Superoxide Dismutases, and Related Matters. *J Biol Chem*. 1997 Jul 25;272(30):18515-7.
- Fromme P, Jordan P, Krauß N (2001) Structure of photosystem I. *Biochim Biophys Acta - Bioenerg* 1507:5–31.
- García-Calderón M, Betti M, Márquez AJ, et al (2019) The afterglow thermoluminescence band as an indicator of changes in the photorespiratory metabolism of the model legume *Lotus japonicus*. *Physiol Plant* 166:240–250.
- Gebicki JM, Bielski BHJ (1981) Comparison of the Capacities of the Peroxyhydroxyl and the Superoxide Radicals to Initiate Chain Oxidation of Linoleic Acid. *J. Am. Chem. Soc* 103:7020–7022.
- Gechev TS, Van Breusegem F, Stone JM, et al (2006) Reactive oxygen species as signals that modulate plant stress responses and programmed cell death. *BioEssays* 28:1091–1101.
- Gombos Z, Kanervo E, Tsvetkova N, et al (1997) Genetic Enhancement of the Ability to Tolerate Photoinhibition by Introduction of Unsaturated Bonds into Membrane Glycerolipids. *Plant Physiol* 115:551–559.
- Gong H (1994) Light-dependent degradation of the Photosystem II D1 protein is retarded by inhibitors of chloroplast transcription and translation: possible involvement of a chloroplast-encoded proteinase. *Biochim Biophys Acta - Bioenerg* 1188:422–426.
- Greer DH, Berry JA, Björkman O (1986) Photoinhibition of photosynthesis in intact bean leaves: role of light and temperature, and requirement for chloroplast-protein synthesis during recovery. *Planta* 168:253–260.
- Havaux M (1996) Short-term responses of Photosystem I to heat stress. *Photosynth Res* 47:85–97.

- Havaux M (1994) Temperature-dependent modulation of the photoinhibition-sensitivity of photosystem II in *Solanum tuberosum* leaves. *Plant Cell Physiol* 35:757–766.
- Havaux M, Rumeau D, Ducruet JM (2005) Probing the FQR and NDH activities involved in cyclic electron transport around Photosystem I by the “afterglow” luminescence. *Biochim Biophys Acta - Bioenerg* 1709:203–213.
- Haldimann P, Tsimilli-Michael M (2005) Non-photochemical quenching of chlorophyll a fluorescence by oxidised plastoquinone: New evidences based on modulation of the redox state of the endogenous plastoquinone pool in broken spinach chloroplasts. *Biochim Biophys Acta - Bioenerg* 1706:239–249.
- He Z, Zheng F, Wu Y, et al (2015) NDH-1L interacts with ferredoxin via the subunit NdhS in *Thermosynechococcus elongatus*. *Photosynth Res* 126:341–349.
- Hideg E, Kálai T, Hideg K, Vass I (1998) Photoinhibition of photosynthesis in vivo results in singlet oxygen production detection via nitroxide-induced fluorescence quenching in broad bean leaves. *Biochemistry* 37:11405–11411.
- Hope AB (2000) Electron transfers amongst Cytochrome f, Plastocyanin and Photosystem I: Kinetics and mechanisms. *Biochim Biophys Acta - Bioenerg* 1456:5–26.
- Hurry VM, Huner NP (1992) Effect of cold hardening on sensitivity of winter and spring wheat leaves to short-term photoinhibition and recovery of photosynthesis. *Plant Physiol* 100:1283–1290.
- Hsu BD, Lee JY (1995) Fluorescence quenching by plastoquinone in an oxygen-evolving photosystem-II-enriched preparation. *J Photochem Photobiol B Biol* 30:57–61.
- Inoue S, Ejima K, Iwai E, et al (2011) Protection by α -tocopherol of the repair of Photosystem II during photoinhibition in *Synechocystis* sp. PCC 6803. *Biochim Biophys Acta - Bioenerg* 1807:236–241.
- Ivanov AG, Hurry V, Sane P V., et al (2008) Reaction centre quenching of excess light energy and photoprotection of Photosystem II. *J Plant Biol* 51:85–96.
- Jahns P, Depka B, Trebst A (2000) Xanthophyll cycle mutants from *Chlamydomonas reinhardtii* indicate a role for zeaxanthin in the D1 protein turnover. *Plant Physiol Biochem* 38:371–376.

Janda T, Szalai G, Páldi E (2001) Thermoluminescence investigation of low temperature stress in maize. *Photosynthetica* 38:635–639.

Janda T, Szalai G, Papp N, et al (2004) Effects of Freezing on Thermoluminescence in Various Plant Species. *Photochem Photobiol* 80:525–530.

Jegerschöld C, Virgin I, Styring S (1990) Light-dependent degradation of the D1 protein in Photosystem II is accelerated after inhibition of the water splitting reaction. *Biochemistry* 29:6179–6186.

Jimbo H, Noda A, Hayashi H, et al (2013) Expression of a highly active catalase VktA in the cyanobacterium *Synechococcus elongatus* PCC 7942 alleviates the photoinhibition of Photosystem II. *Photosynth Res* 117:509–515.

Joliot P (2003) Period-four oscillations of the flash-induced oxygen formation in photosynthesis. *Photosynth Res* 76:65–72.

Kapoor, S., and Varshney, L. (1997). Redox reactions of chloramphenicol and some aryl peroxy radicals in aqueous solutions: A pulse radiolytic study. *J. Phys. Chem. A* 101, 7778–7782.

Kale R, Hebert AE, Frankel LK, et al (2017) Amino acid oxidation of the D1 and D2 proteins by oxygen radicals during photoinhibition of Photosystem II. *Proc Natl Acad Sci USA* 114:2988–2993.

Kamiya N, Shen JR (2003) Crystal structure of oxygen-evolving Photosystem II from *Thermosynechococcus vulcanus* at 3.7-Å resolution. *Proc Natl Acad Sci USA* 100:98–103.

Kaneko T, Sato S, Kotani H, et al (1996) Sequence analysis of the genome of the unicellular cyanobacterium *Synechocystis* sp. strain PCC6803. II. Sequence determination of the entire genome and assignment of potential protein-coding regions (supplement). *DNA Res* 3:185–209.

Karapetyan N V (2008) Protective dissipation of excess absorbed energy by photosynthetic apparatus of cyanobacteria: role of antenna terminal emitters. *Photosynth Res* 97:195.

Kettunen R, Tyystjärvi E, Aro E-M (1991) D1 protein degradation during photoinhibition of intact leaves: a modification of the D1 protein precedes degradation. *FEBS Lett* 290:153–156.

- Kofer W, Koop HU, Wanner G, Steinmüller K (1998) Mutagenesis of the genes encoding subunits A, C, H, I, J and K of the plastid NAD(P)H-plastoquinone-oxidoreductase in tobacco by polyethylene glycol-mediated plastome transformation. *Mol Gen Genet* 258:166–173.
- Komenda J (1998) Photosystem II photoinactivation and repair in the *Scenedesmus* cells treated with herbicides DCMU and BNT and exposed to high irradiance. *Photosynthetica* 35:477–480.
- Komenda J, Koblížek M, Masojídek J (1999) The regulatory role of Photosystem II photoinactivation and de novo protein synthesis in the degradation and exchange of two forms of the D1 protein in the cyanobacterium *Synechococcus* PCC 7942. *J Photochem Photobiol B Biol* 48:114–119.
- Komenda J, Masojídek J (1998) The effect of Photosystem II inhibitors DCMU and BNT on the high-light induced D1 turnover in two cyanobacterial strains *Synechocystis* PCC 6803 and *Synechococcus* PCC 7942. *Photosynth Res* 57:193–202.
- Komenda J, Tichý M, Prášil O, et al (2007) The exposed N-terminal tail of the D1 subunit is required for rapid D1 degradation during Photosystem II repair in *Synechocystis* sp PCC 6803. *Plant Cell* 19:2839–2854.
- Komenda J, Barber J (1995) Comparison of psbO and psbH deletion mutants of *Synechocystis* PCC 6803 indicates that degradation of D1 protein is regulated by the QB site and dependent on protein synthesis. *Biochemistry* 34:9625–9631.
- Kodru S, Rehman AU, Vass I (2020) Chloramphenicol enhances Photosystem II photodamage in intact cells of the cyanobacterium *Synechocystis* PCC 6803. *Photosynth Res* 145:227–235.
- Kodru S, Sass L, Patil P, et al (2021) Identification of the AG afterglow thermoluminescence band in the cyanobacterium *Synechocystis* PCC 6803. *Physiol Plant* 171:291–300.
- Krieger-Liszkay A (2005) Singlet oxygen production in photosynthesis. *J Exp Bot* 56:337–346.
- Krieger-Liszkay A, Fufezan C, Trebst A (2008) Singlet oxygen production in photosystem II and related protection mechanism. *Photosynth Res* 98:551–564

- Krieger A, Bolte S, Dietz KJ, Ducruet JM (1998) Thermoluminescence studies on the facultative crassulacean-acid-metabolism plant *Mesembryanthemum crystallinum* L. *Planta* 205:587–594.
- Kruk J, Holländer-Czytko H, Oettmeier W, Trebst A (2005) Tocopherol as singlet oxygen scavenger in photosystem II. *J Plant Physiol* 162:749–757
- Kusama Y, Inoue S, Jimbo H, et al (2015) Zeaxanthin and Echinonone Protect the Repair of Photosystem II from Inhibition by Singlet Oxygen in *Synechocystis* sp. PCC 6803. *Plant Cell Physiol* 56:906–916.
- Kyle DJ, Ohad I, Arntzen CJ (1984) Membrane protein damage and repair: Selective loss of a quinone-protein function in chloroplast membranes. *Proc Natl Acad Sci* 81:4070–4074.
- Li M, Calteau A, Semchonok DA, et al (2019) Physiological and evolutionary implications of tetrameric photosystem I in cyanobacteria. *Nat Plants* 5:1309–1319.
- Lee Y, Rubio MC, Alassimone J, Geldner N (2013) A mechanism for localized lignin deposition in the endodermis. *Cell* 153:402–412.
- Leister D (2019) Piecing the puzzle together: the central role of reactive oxygen species and redox hubs in chloroplast retrograde signaling. *Antioxid Redox Signal* 30:1206–1219
- Liu H, Zhang H, Niedzwiedzki DM, Prado M, He G, Gross ML, Blankenship RE. Phycobilisomes supply excitations to both photosystems in a megacomplex in cyanobacteria. *Science*. 2013 Nov 29;342(6162):1104-7.
- Liu Z, Yan H, Wang K, et al (2004) Crystal structure of spinach major light-harvesting complex at 2.72 Å resolution. *Nature* 428:287–292.
- Luciński R, Jackowski G (2006) The structure, functions and degradation of pigment-binding proteins of photosystem II. *Acta Biochim Pol* 53:693–708.
- Long SP, Humphries S, Falkowski PG (1994) Photoinhibition of Photosynthesis in Nature. *Annu Rev Plant Physiol Plant Mol Biol* 45:633–662.
- Mano J, Miyake C, Schreiber U, Asada K (1995) Photoactivation of the electron flow from NADPH to plastoquinone in spinach chloroplasts. *Plant Cell Physiol* 36:1589–1598.

- Maxwell DP, Falk S, Huner NPA (1995) Photosystem II Excitation Pressure and Development of Resistance to Photoinhibition (I. Light-Harvesting Complex II Abundance and Zeaxanthin Content in *Chlorella vulgaris*). *Plant Physiol* 107:687–694.
- Macpherson, A. N., Telfer, A., Barber, J., Truscott, T. G. (1993) Direct detection of singlet oxygen from isolated Photosystem II reaction centres. *Biochim. Biophys. Acta* 1143:301-309.
- Martin Re, Thomas Dj, Tucker De, Herbert Sk (1997) The effects of photooxidative stress on Photosystem I measured in vivo in *Chlamydomonas*. *Plant Cell Environ* 20:1451–1461.
- Martínez-Reyes I, Cuezva JM (2014) The H⁺-ATP synthase: A gate to ROS-mediated cell death or cell survival. *Biochim Biophys Acta - Bioenerg* 1837:1099–1112.
- Meetam M, Keren N, Ohad I, Pakrasi HB (1999) The PsbY protein is not essential for oxygenic photosynthesis in the cyanobacterium *Synechocystis* sp. PCC 6803. *Plant Physiol* 121:1267–1272.
- Melis A (1999) Photosystem-II damage and repair cycle in chloroplasts: what modulates the rate of photodamage in vivo? *Trends Plant Sci* 4:130–135.
- Mi H, Endo T, Ogawa T, Asada K (1995) Thylakoid Membrane-Bound, NADPH-Specific Pyridine Nucleotide Dehydrogenase Complex Mediates Cyclic Electron Transport in the Cyanobacterium *Synechocystis* sp. PCC 6803. *Plant Cell Physiol* 36:661–668.
- Mi H, Endo T, Schreiber U, et al (1992) Electron donation from cyclic and respiratory flows to the photosynthetic intersystem chain is mediated by pyridine nucleotide dehydrogenase in the Cyanobacterium *Synechocystis* PCC 6803. *Plant Cell Physiol* 33:1233–1237.
- Mimuro M, Kikuchi H, Murakami A (1999) Structure and unction of Phycobilisomes BT - Concepts in Photobiology: Photosynthesis and Photomorphogenesis. In: Singhal GS, Renger G, Sopory SK, et al. (eds). Springer Netherlands, Dordrecht, pp 104–135
- Miranda T, Ducruet JM (1995) Effects of dark- and light-induced proton gradients in thylakoids on the Q and B thermoluminescence bands. *Photosynth Res* 43:251–262.
- Mitchell P (1975) The protonmotive Q cycle: A general formulation. *FEBS Lett* 59:137–139.
- Mitchell P (1961) Coupling of Phosphorylation to Electron and Hydrogen Transfer by a Chemi-Osmotic type of Mechanism. *Nature* 191:144–148.

- Miyake C (2010) Alternative Electron Flows (Water–Water Cycle and Cyclic Electron Flow around PSI) in Photosynthesis: Molecular Mechanisms and Physiological Functions. *Plant Cell Physiol* 51:1951–1963.
- Miyao M, Ikeuchi M, Yamamoto N, Ono T (1995) Specific Degradation of the D1 Protein of Photosystem II by Treatment with Hydrogen Peroxide in Darkness: Implications for the Mechanism of Degradation of the D1 Protein under Illumination. *Biochemistry* 34:10019–10026.
- Müller P, Li X-P, Niyogi KK (2001) Non-Photochemical Quenching. A Response to Excess Light Energy. *Plant Physiol* 125:1558 LP – 1566.
- Mulo P, Pursiheimo S, Hou CX, et al (2003) Multiple effects of antibiotics on chloroplast and nuclear gene expression. *Funct Plant Biol* 30:1097–1103.
- Mulo P, Sirpiö S, Suorsa M, Aro EM (2008) Auxiliary proteins involved in the assembly and sustenance of Photosystem II. *Photosynth Res* 98:489–501.
- Munekage Y, Hojo M, Meurer J, et al (2002) PGR5 is involved in cyclic electron flow around Photosystem I and is essential for photoprotection in Arabidopsis. *Cell* 110:361–371.
- Murata N, Nishiyama Y (2018) ATP is a driving force in the repair of Photosystem II during photoinhibition. *Plant Cell Environ* 41:285–299.
- Murata N, Takahashi S, Nishiyama Y, Allakhverdiev SI (2007) Photoinhibition of Photosystem II under environmental stress. *Biochim. Biophys. Acta - Bioenerg.* 1767:414–421.
- Montgomery BL (2014) The Regulation of Light Sensing and Light-Harvesting Impacts the Use of Cyanobacteria as Biotechnology Platforms . *Front. Bioeng. Biotechnol.* 2:22
- Nagao R, Tomo T, Narikawa R, et al (2016) Conversion of Photosystem II dimer to monomers during photoinhibition is tightly coupled with decrease in oxygen-evolving activity in the diatom *Chaetoceros gracilis*. *Photosynth Res* 130:83–91.
- Nakamoto H, Sundblad L-G, Gardeström P, Sundbom E (1988) Far-red stimulated long-lived luminescence from barley protoplasts. *Plant Sci* 55: 1–7

- Nikkanen L, Solymosi D, Jokel M (2021) Regulatory electron transport pathways of photosynthesis in cyanobacteria and microalgae: Recent advances and biotechnological prospects. *Physiol Plant* 1–12.
- Nishiyama Y, Allakhverdiev SI, Murata N (2005) Inhibition of the repair of Photosystem II by oxidative stress in cyanobacteria. *Photosynth Res* 84:1–7.
- Nishiyama Y, Allakhverdiev SI, Yamamoto H, et al (2004) Singlet oxygen inhibits the repair of Photosystem II by suppressing the translation elongation of the D1 protein in *Synechocystis* sp. PCC 6803. *Biochemistry* 43:11321–11330.
- Nixon PJ, Barker M, Boehm M, et al (2005) FtsH-mediated repair of the Photosystem II complex in response to light stress. *J Exp Bot* 56:357–363.
- Nixon PJ, Michoux F, Yu J, et al (2010) Recent advances in understanding the assembly and repair of Photosystem II. *Ann Bot* 106:1–16.
- Nobel PS (2005) 5 - Photochemistry of Photosynthesis. In: Nobel PS (ed) *Physicochemical and Environmental Plant Physiology (Third Edition)*, Third Edit. Academic Press, Burlington, pp 219–266.
- Ogawa T (1991) A gene homologous to the subunit-2 gene of NADH dehydrogenase is essential to inorganic carbon transport of *Synechocystis* PCC 6803. *Proc Natl Acad Sci USA* 88:4275–4279.
- Ogilby PR (2010) Singlet oxygen: there is still something new under the sun, and it is better than ever. *Photochem Photobiol Sci* 9:1543–1560.
- Ögren E, Sjöström M (1990) Estimation of the effect of photoinhibition on the carbon gain in leaves of a willow canopy. *Planta* 181:560–567.
- Ohad I, Kyle DJ, Arntzen CJ (1984) Membrane protein damage and repair: removal and replacement of inactivated 32-kilodalton polypeptides in chloroplast membranes. *J Cell Biol* 99:481–485.
- Okada K, Satoh K, Katoh S (1991) Chloramphenicol is an inhibitor of photosynthesis. *FEBS Lett* 295:155–158.

- Ortega JM, Roncel M (2021) The afterglow photosynthetic luminescence. *Physiol Plant* 171:268–276.
- Osmond CB, Ramus J, Levavasseur G, et al (1993) Fluorescence quenching during photosynthesis and photoinhibition of *Ulva rotundata* Blid. *Planta* 190:97–106.
- Oszyczka A, Moser CC, Dutton PL (2005) Fixing the Q cycle. *Trends Biochem Sci* 30:176–182.
- Owens TG (1996) Processing of Excitation Energy by Antenna Pigments BT -Photosynthesis and the Environment. In: Baker NR (ed). Springer Netherlands, Dordrecht, pp 1–23
- Paumard P, Vaillier J, Coulary B, et al (2002) The ATP synthase is involved in generating mitochondrial cristae morphology. *EMBO J* 21:221–230.
- Peltier G, Aro E-M, Shikanai T (2016) NDH-1 and NDH-2 Plastoquinone Reductases in Oxygenic Photosynthesis. *Annu Rev Plant Biol* 67:55–80.
- Peretó J (2011) Anoxygenic Photosynthesis BT - Encyclopedia of Astrobiology. In: Gargaud M, Amils R, Quintanilla JC, et al. (eds). Springer Berlin Heidelberg, Berlin, Heidelberg, p 46
- Pospíšil P (2009) Production of reactive oxygen species by photosystem II. *Biochim Biophys Acta - Bioenerg* 1787:1151–1160.
- Pospíšil P (2012) Molecular mechanisms of production and scavenging of reactive oxygen species by Photosystem II. *Biochim Biophys Acta - Bioenerg* 1817:218–231.
- Pospíšil P, Prasad A, Rác M (2019) Mechanism of the formation of Electronically Excited Species by Oxidative Metabolic Processes: Role of Reactive Oxygen Species. *Biomolecules* 9: (7):258.
- Pospíšil P, Šnyrychová I, Kruk J, et al (2006) Evidence that cytochrome b₅₅₉ is involved in superoxide production in Photosystem II: Effect of synthetic short-chain plastoquinones in a cytochrome b₅₅₉ tobacco mutant. *Biochem J* 397:321–327.
- Powles SB (1984) Photoinhibition of Photosynthesis Induced by Visible Light. *Annu Rev Plant Physiol* 35:15–44.
- Prasil O, Adir N, Ohad I (1992) Dynamics of Photosystem II: mechanism of photoinhibition and recovery process. *Top Photosynth* 11:295–348

- Pribil M, Sandoval-Ibáñez O, Xu W, et al (2018) Fine-tuning of photosynthesis requires CURVATURE THYLAKOID1-mediated thylakoid plasticity. *Plant Physiol* 176:2351–2364.
- Rast A, Heinz S, Nickelsen J (2015) Biogenesis of thylakoid membranes. *Biochim. Biophys. Acta - Bioenerg.* 1847:821–830
- Raszewski G, Diner BA, Schlodder E, Renger T (2008) Spectroscopic Properties of Reaction Center Pigments in Photosystem II Core Complexes: Revision of the Multimer Model. *Biophys J* 95:105–119.
- Rehman AU (2016) PhD Thesis. Detection of singlet oxygen production and its relation to Photosystem II photodamage in intact cyanobacteria and microalgae.
- Rehman AU, Cser K, Sass L, Vass I (2013) Characterization of singlet oxygen production and its involvement in photodamage of Photosystem II in the cyanobacterium *Synechocystis* PCC 6803 by histidine-mediated chemical trapping. *Biochim Biophys Acta - Bioenerg* 1827:689–698.
- Rehman AU, Kodru S, Vass I (2016) Chloramphenicol mediates superoxide production in photosystem II and enhances its photodamage in isolated membrane particles. *Front Plant Sci* 7:1–5.
- Renger G, Renger T (2008) Photosystem II: The machinery of photosynthetic water splitting. *Photosynth Res* 98:53–80.
- Repetto G, Zurita JL, Roncel M, Ortega JM (2015) Thermoluminescence as a complementary technique for the toxicological evaluation of chemicals in photosynthetic organisms. *Aquat Toxicol* 158:88–97.
- Rodrigues MA, Dos Santos CP, Young AJ, et al (2002) A smaller and impaired xanthophyll cycle makes the deep sea macroalgae *Laminaria abyssalis* (phaeophyceae) highly sensitive to daylight when compared with shallow water *Laminaria digitata*. *Journal of Phycology*, 38:939–947.
- Roncel M, González-Rodríguez AA, Naranjo B, et al (2016) Iron deficiency induces a partial inhibition of the photosynthetic electron transport and a high sensitivity to light in the diatom *Phaeodactylum tricorutum*. *Front Plant Sci* 7:1–14.

- Roncel M, Yruela I, Kirilovsky D, et al (2007) Changes in photosynthetic electron transfer and state transitions in an herbicide-resistant D1 mutant from soybean cell cultures. *Biochim Biophys Acta - Bioenerg* 1767:694–702.
- Ruban A V, Berera R, Iliaia C et al (2007) Identification of a mechanism of photoprotective energy dissipation in higher plants. *Nature* 450:575–578.
- Rutherford AW, Crofts AR, Inoue Y (1982) Thermoluminescence as a probe of Photosystem II photochemistry. The origin of the flash-induced glow peaks. *BBA - Bioenerg* 682:457–465.
- Sae-Tang P, Hihara Y, Yumoto I, et al (2016) Overexpressed Superoxide Dismutase and Catalase Act Synergistically to Protect the Repair of PSII during Photoinhibition in *Synechococcus elongatus* PCC 7942. *Plant Cell Physiol* 57:1899–1907.
- Sánchez-Aragó M, García-Bermúdez J, Martínez-Reyes I, et al (2013) Degradation of IF1 controls energy metabolism during osteogenic differentiation of stem cells. *EMBO Rep* 14:638–644.
- Sánchez-Cenizo L, Formentini L, Aldea M, et al (2010) Up-regulation of the ATPase Inhibitory Factor 1 (IF1) of the Mitochondrial H⁺-ATP Synthase in Human Tumors Mediates the Metabolic Shift of Cancer Cells to a Warburg Phenotype*. *J Biol Chem* 285:25308–25313.
- Santana-Sánchez A, Solymosi D, Mustila H, et al (2019) Flv1-4 proteins function in versatile combinations in O₂ photoreduction in cyanobacteria. *bioRxiv* 1–22.
- Saradhi PP, Suzuki I, Katoh A, et al (2000) Protection against the photo-induced inactivation of the Photosystem II complex by abscisic acid. *Plant Cell Environ* 23:711–718.
- Sass L, Spetea C, Máté Z, et al (1997) Repair of UV-B induced damage of Photosystem II via de novo synthesis of the D1 and D2 reaction centre subunits in *Synechocystis* sp. PCC 6803. *Photosynth Res* 54:55–62.
- Scherer S (1990) Do photosynthetic and respiratory electron transport chains share redox proteins? *Trends Biochem Sci* 15:458–462.
- Schirrmeister BE, Gugger M, Donoghue PCJ (2015) Cyanobacteria and the Great Oxidation Event: Evidence from genes and fossils. *Palaeontology* 58:769–785.

- Schuller JM, Birrell JA, Tanaka H, et al (2019) Structural adaptations of photosynthetic complex I enable ferredoxin-dependent electron transfer. *Science* vol 363:257–260.
- Sedoud A, López-Igual R, Rehman AU, et al (2014) The cyanobacterial photoactive orange carotenoid protein is an excellent singlet oxygen quencher. *Plant Cell* 26:1781–1791.
- Shen Gaozhong, Boussiba S, Vermaas WFJ (1993) *Synechocystis* sp PCC 6803 strains lacking Photosystem I and phycobilisome function. *Plant Cell* 5:1853–1863.
- Shen J-R, Henmi T, Kamiya N (2008) Structure and Function of Photosystem II. *Photosynth. Protein Complexes* 83–106.
- Shibamoto T, Kato Y, Sugiura M, Watanabe T (2009) Redox Potential of the Primary Plastoquinone Electron Acceptor Q_A in Photosystem II from *Thermosynechococcus elongatus* Determined by Spectroelectrochemistry. *Biochemistry* 48:10682–10684.
- Shikanai T, Endo T, Hashimoto T, et al (1998) Directed disruption of the tobacco *ndhB* gene impairs cyclic electron flow around photosystem I. *Proc Natl Acad Sci USA* 95:9705–9709.
- Sicora C, Máté Z, Vass I (2003) The interaction of visible and UV-B light during photodamage and repair of Photosystem II. *Photosynth Res* 75:127–137.
- Stamenković M, Hanelt D (2013) Protection strategies of *Cosmarium* strains (Zygnematophyceae, Streptophyta) isolated from various geographic regions against excessive Photosynthetically Active Radiation. *Photochem Photobiol* 89:900–910.
- Stapel D, Kruse E, Kloppstech K (1993) The protective effect of heat shock proteins against photoinhibition under heat shock in barley (*Hordeum vulgare*). *J Photochem Photobiol B Biol* 21:211–218.
- Strand DD, Fisher N, Kramer DM (2017) The higher plant plastid NAD(P)H dehydrogenase-like complex (NDH) is a high efficiency proton pump that increases ATP production by cyclic electron flow. *J Biol Chem* 292:11850–11860.
- Strasserf RJ, Srivastava A, Govindjee (1995) polyphasic chlorophyll a fluorescence transient in plants and cyanobacteria. *Photochem Photobiol* 61:32–42.
- Styring S, Rutherford AW (1987) In the oxygen-evolving complex of photosystem II the S_0 state is oxidized to the S_1 state by D^+ (signal II_{slow}). *Biochemistry* 26:2401–2405.

- Styring S, Sjöholm J, Mamedov F (2012) Two tyrosines that changed the world: Interfacing the oxidizing power of photochemistry to water splitting in photosystem II. *Biochim Biophys Acta - Bioenerg* 1817:76–87.
- Sundblad L-G, Sjöström M, Malmberg G, Öquist G (1990) Prediction of frost hardiness in seedlings of Scots pine (*Pinussylvestris*) using multivariate analysis of chlorophyll a fluorescence and luminescence kinetics. *Can J For Res* 20:592–597.
- Takahashi S, Milward SE, Yamori W, et al (2010) The Solar Action Spectrum of Photosystem II Damage. *Plant Physiol* 153:988–993.
- Takahashi S, Murata N (2005) Interruption of the Calvin cycle inhibits the repair of Photosystem II from photodamage. *Biochim Biophys Acta - Bioenerg* 1708:352–361.
- Takahashi S, Yoshioka-Nishimura M, Nanba D, Badger MR (2013) Thermal Acclimation of the Symbiotic Alga *Symbiodinium* spp. Alleviates Photobleaching under Heat Stress. *Plant Physiol* 161:477–485.
- Telfer A (2005) Too much light? How β -carotene protects the Photosystem II reaction centre. *Photochem Photobiol Sci* 4:950–956.
- Telfer A (2014) Singlet oxygen production by PSII under light stress: Mechanism, detection and the protective role of β -carotene. *Plant Cell Physiol* 55:1216–1223.
- Telfer A, Bishop SM, Phillips D, Barber J (1994) Isolated photosynthetic reaction center of Photosystem II as a sensitizer for the formation of singlet oxygen. Detection and quantum yield determination using a chemical trapping technique. *J Biol Chem* 269:13244–13253.
- Tikkanen M, Aro E-M (2014) Integrative regulatory network of plant thylakoid energy transduction. *Trends Plant Sci* 19:10–17.
- Tikkanen M, Mekala NR, Aro E-M (2014) Photosystem II photoinhibition-repair cycle protects Photosystem I from irreversible damage. *Biochim Biophys Acta* 1837:210–215.
- Thomas DJ, Thomas J, Youderian PA, Herbert SK (2001) Photoinhibition and light-induced cyclic electron transport in *ndhB*- and *psaE*- mutants of *Synechocystis* sp. PCC 6803. *Plant Cell Physiol* 42:803–812.

- Torrado A, Ramírez-Moncayo C, Navarro JA, et al (2019) Cytochrome c6 is the main respiratory and photosynthetic soluble electron donor in heterocysts of the cyanobacterium *Anabaena* sp. PCC 7120. *Biochim Biophys Acta - Bioenerg* 1860:60–68.
- Trebst A, Soll-Bracht E (1996) Cycloheximide retards high light driven D1 protein degradation in *Chlamydomonas reinhardtii*. *Plant Sci* 115:191–197.
- Tyystjärvi E, Ali-Yrkkö K, Kettunen R, Aro E-M (1992) Slow Degradation of the D1 Protein Is Related to the Susceptibility of Low-Light-Grown Pumpkin Plants to Photoinhibition, *Plant Physiol* 100:1310–1317.
- Tyystjärvi E, Aro EM (1996) The rate constant of photoinhibition, measured in lincomycin-treated leaves, is directly proportional to light intensity. *Proc Natl Acad Sci USA* 93:2213–2218.
- Ueno M, Sae-Tang P, Kusama Y, et al (2016) Moderate Heat Stress Stimulates Repair of Photosystem II During Photoinhibition in *Synechocystis* sp. PCC 6803. *Plant Cell Physiol* 57:2417–2426.
- Umena Y, Kawakami K, Shen JR, Kamiya N (2011) Crystal structure of oxygen-evolving Photosystem II at a resolution of 1.9Å. *Nature* 473:55–60.
- Vass I (2012) Molecular mechanisms of photodamage in the Photosystem II complex. *Biochim Biophys Acta - Bioenerg* 1817:209–217.
- Vass I (2011) Role of charge recombination processes in photodamage and photoprotection of the Photosystem II complex. *Physiol Plant* 142:6–16.
- Vass, I. (2019) The role of Singlet Oxygen in Photoinhibition of Photosystem II. in *Oxygen Production and Reduction in Artificial and Natural Systems*, J. Barber, P. Nixon and A.V. Ruban eds., World Scientific Publishers. pp. 91-118
- Vass I, Aro E-M (2008) Chapter 10 Photoinhibition of Photosynthetic Electron Transport. *The Royal Society of Chemistry*, pp 393–425
- Vass I, Chapman DJ, Barber J (1989) Thermoluminescence properties of the isolated Photosystem two reaction centre. *Photosynth Res* 22:295–301.

Vass I, Cser K (2009) Janus-faced charge recombinations in Photosystem II photoinhibition. *Trends Plant Sci* 14:200–205.

Vass I, Horváth G, Herczeg T, Demeter S (1981) Photosynthetic energy conservation investigated by thermoluminescence. Activation energies and half-lives of thermoluminescence bands of chloroplasts determined by mathematical resolution of glow curves. *Biochim Biophys Acta - Bioenerg* 634:140–152.

Vass I, Ono T aki, Inoue Y (1987) Removal of 33 kDa extrinsic protein specifically stabilizes the $S_2Q_A^-$ charge pair in photosystem II. *FEBS Lett* 211:215–220.

Vass I, Styring S, Hundal T, et al (1992) Reversible and irreversible intermediates during photoinhibition of Photosystem II: stable reduced QA species promote chlorophyll triplet formation. *Proc Natl Acad Sci USA* 89:1408–1412.

Vass I, Sass L, Spetea C, et al (1996) UV-B-Induced Inhibition of Photosystem II Electron Transport Studied by EPR and Chlorophyll Fluorescence. Impairment of Donor and Acceptor Side Components. *Biochemistry* 35:8964–8973.

Vass I, Turcsányi E, Touloupakis E, et al (2002) The Mechanism of UV-A Radiation-Induced Inhibition of Photosystem II Electron Transport Studied by EPR and Chlorophyll Fluorescence. *Biochemistry* 41:10200–10208.

Vavilin D V, Polynov VA, Matorin DN, Venediktov PS (1995) Sublethal Concentrations of Copper Stimulate Photosystem II Photoinhibition in *Chlorella pyrenoidosa*. *J Plant Physiol* 146:609–614.

Vincent WF (2007) Cold Tolerance in Cyanobacteria and Life in the Cryosphere BT - Algae and Cyanobacteria in Extreme Environments. In: Seckbach J (ed). Springer Netherlands, Dordrecht, pp 287–301

Vonshak A, Torzillo G, Tomaseli L (1994) Use of chlorophyll fluorescence to estimate the effect of photoinhibition in outdoor cultures of *Spirulina platensis*. *J Appl Phycol* 6:31–34.

Yamamoto H, Miyake C, Dietz KJ, et al (1999) Thioredoxin peroxidase in the Cyanobacterium *Synechocystis* sp. PCC 6803. *FEBS Lett* 447:269–273.

Yamamoto H, Peng L, Fukao Y, Shikanai T (2011) An Src homology 3 domain-like fold protein forms a ferredoxin binding site for the chloroplast NADH dehydrogenase-like complex in Arabidopsis. *Plant Cell* 23:1480–1493.

Yamanaka G, Glazer AN, Williams RC (1978) Cyanobacterial phycobilisomes. Characterization of the phycobilisomes of *Synechococcus* sp. 6301. *J Biol Chem* 253:8303–8310.

Yamanaka S, Isobe H, Kanda K, et al (2011) Possible mechanisms for the O-O bond formation in oxygen evolution reaction at the $\text{CaMn}_4\text{O}_5(\text{H}_2\text{O})_4$ cluster of PSII refined to 1.9 Å X-ray resolution. *Chem Phys Lett* 511:138–145.

Zavafer A, Koinuma W, Chow WS, et al (2017) Mechanism of photodamage of the oxygen evolving Mn Cluster of Photosystem II by excessive light energy. *Sci Rep* 7, 7604.

Zhang L-T, Zhang Z-S, Gao H-Y, et al (2011) Mitochondrial alternative oxidase pathway protects plants against photoinhibition by alleviating inhibition of the repair of photodamaged PSII through preventing formation of reactive oxygen species in *Rumex* K-1 leaves. *Physiol Plant* 143:396–407.

Zhang L, He M, Liu J, Li L (2015) Role of the mitochondrial alternative oxidase pathway in hydrogen photoproduction in *Chlorella protothecoides*. *Planta* 241:1005—1014.

Zhang L, Niyogi KK, Baroli I, et al (1997) DNA insertional mutagenesis for the elucidation of a Photosystem II repair process in the green alga *Chlamydomonas reinhardtii*. *Photosynth Res* 53:173–184.

Zhang L, Paakkarinen V, Van Wijk KJ, Aro EM (2000) Biogenesis of the chloroplast-encoded D1 protein: Regulation of translation elongation, insertion, and assembly into Photosystem II. *Plant Cell* 12:1769–1781.

Zhao J, Gao F, Fan DY, et al (2018) NDH-1 is important for Photosystem I function of *synechocystis* sp. Strain PCC 6803 under environmental stress conditions. *Front Plant Sci* 8:1–10.

6. Summary

- Our data show that chloramphenicol (CAP) can accept electrons at the acceptor side of Photosystem II, before the Q_B site, and deliver them to molecular oxygen leading to superoxide production. In addition, the presence of CAP enhances photodamage of Photosystem II electron transport in isolated thylakoids and BBY particles, which effect is reversible by superoxide dismutase (Rehman et al. 2016) showing that CAP induces superoxide dependent photodamage.
- Our results also show that in intact *Synechocystis* PCC 6803 cells the rate of PSII photodamage was significantly enhanced by CAP, at the usually applied $200 \mu\text{g mL}^{-1}$ concentration, relative to that obtained in the presence of lincomycin. These data provide evidence for the previously indicated damaging effect of PSII activity by CAP (Rehman 2016). The CAP-induced enhancement of photodamage was observed not only in wild-type *Synechocystis* 6803, which contains both Photosystem I (PSI) and PSII, but also in a PSI-less mutant which contains only PSII. Importantly, the rate of PSII photodamage was also enhanced by the absence of PSI when compared to that in the wild-type strain under all conditions studied here, i.e., without addition and in the presence of protein synthesis inhibitors.
- The so-called afterglow, AG, thermoluminescence (TL) band is a useful indicator of the presence of cyclic electron flow (CEF), which is mediated by the NADH dehydrogenase-like (NDH) complex in higher plants. Although NDH-dependent CEF occurs also in cyanobacteria, the AG band has previously not been found in these organisms. We tested various experimental conditions and could identify a TL component with ca. $+40 \text{ }^\circ\text{C}$ peak temperature in *Synechocystis* PCC 6803 cells, which were illuminated by far-red (FR) light at around $-10 \text{ }^\circ\text{C}$. The $+40 \text{ }^\circ\text{C}$ band could be observed when WT cells were grown under ambient air level CO_2 , but was absent in the M55 mutant, which is deficient in the NDH-1 complex. These experimental observations match the characteristics of the AG band of higher plants. Therefore, we conclude that the newly identified $+40 \text{ }^\circ\text{C}$ TL component in *Synechocystis* PCC 6803 is the cyanobacterial counterpart of the plant AG band and originates from NDH-1-mediated CEF. The cyanobacterial AG band was most efficiently induced when FR illumination was applied at $-10 \text{ }^\circ\text{C}$ and its contribution to the total TL intensity

declined when cells were illuminated above and below this temperature. Based on this phenomenon we also conclude that CEF is blocked by low temperatures at two different sites in *Synechocystis* PCC 6803: (1) Below -10 °C at the level of NDH-1 and (2) below -30 °C at the donor or acceptor side of Photosystem I (Kodru et al. 2021).

- We conclude that chloramphenicol enhances photodamage mostly by its interaction with PSII, leading probably to superoxide production. The presence of PSI is also an important regulatory factor of PSII photodamage most likely via decreasing excitation pressure on PSII (Kodru et al. 2020). Identification of the AG opens new ways to study the role of cyclic electron transport in photoprotection in cyanobacteria.

7.0. Összefoglalás

- Eredményeink szerint a kloramfenikol képes a kettes fotokémiai rendszer (PSII) akceptor oldalán történő elektron felvételre, valószínűleg a feofitin elsődleges akceptortól, és elektronok segítségével oxigén redukálására, azaz szuperoxid (O_2^-) létrehozására. Emellett a kloramfenikol jelenlétében felgyorsul a PSII elektron transzportjának fényindukált gátlása, az ún. fotoinhibíció, izolált tilakoid membránokban és PSII (BBY) komplexekben. Ez a hatás szuperoxid dizmutáz (SOD) hozzáadásával nagyrészt megelőzhető (Rehman és mtsai, 2016), ami azt mutatja, hogy kloramfenikol fénykárosítást felerősítő hatása szuperoxid közvetítésével történik.
- Eredményeink szerint a PSII fénygátlásának sebességét a kloramfenikol intakt *Synechocystis* PCC 6803 sejtekben is felerősíti a szokásosan használt $200 \mu\text{g mL}^{-1}$ koncentráció esetén, ahhoz képest ami linkomicin jelenlétében tapasztalható. Ez az eredmény egyértelmű bizonyítékot ad a kloramfenikol korábban felvetett (Rehman 2016) fénykárosító hatására intakt sejtekben. Ez a jelenség nem csak a vad típusú *Synechocystis* PCC 6803 törzs esetén volt megfigyelhető, amelyben mind a PSII mind a PSI (I-es fotokémiai rendszer) megtalálható, hanem a csak PSII-öt tartalmazó PSI-mentes mutánsokban is. Fontos megjegyezni, hogy a PSI komplex hiánya a fénygátlás sebességének általános felgyorsulását eredményezte a vad típusú törzshöz képest, a kloramfenikol (és más protein szintézis gátlók) hiányában is (Kodru és mtsai 2020).
- Az ún. AG termolumineszcencia (TL) sáv a ciklikus elektron transzport meglétének fontos és hasznos indikátora magasabb rendű növényekben, amit az NDH komplex közvetít. Annak ellenére, hogy NDH-tól függő ciklikus elektron transzport cianobaktériumokban is jelen van az AG TL sávot korábban nem figyelték meg ezekben a szervezetekben. Különböző kísérleti körülmények tesztelésével sikerült kimutatnunk egy $40 \text{ }^\circ\text{C}$ körüli csúcshőmérséklettel rendelkező TL sáv jelenlétét *Synechocystis* PCC 6803-ban. A $40 \text{ }^\circ\text{C}$ -os TL sáv megjelenéséhez távoli vörös fényvel történő megvilágítás, valamint az NDH-1 komplex jelenléte szükséges a *Synechocystis* sejtekben. Ezen tulajdonságok alapján az új $40 \text{ }^\circ\text{C}$ -os TL sávot az NDH által közvetített ciklikus elektron transzportot tükröző AG sáv cianobaktériális megfelelőjének tekinthetjük. Az AG sáv gerjeszthetőségének hőmérséklet függését vizsgálva arra a következtetésre jutottunk, hogy a cianobaktériális ciklikus electron

transzport két különböző alacsony hőmérsékleten gátlódik: $-10\text{ }^{\circ}\text{C}$ alatt az NDH-1 komplexnél, $-30\text{ }^{\circ}\text{C}$ alatt pedig a PSI-nél.

- Eredményeink összegzése alapján: (i) A kloramfenikol elsősorban a PSII-vel való, feltehetően szuperoxid képződést eredményező, kölcsönhatása révén felerősíti a PSII fénygátlását. (ii) A PSI komplex a fénygátlási folyamat fontos szabályzója, mivel funkciója csökkenti a PSII komplexre ható gerjesztési nyomást. (iii) A cianobakteriális AG TL sáv azonosítása új lehetőségeket nyit a ciklikus elektron transzport és az általa biztosított fotoprotekciós hatások vizsgálatára cianobakteriális rendszerekben.

8.0. LIST OF PUBLICATIONS (MTMT ID: 10054575) IF: 14, 9

Publications related to the PhD thesis:

- Kodru S, Rehman AU, Vass I (2020) Chloramphenicol enhances Photosystem II photodamage in intact cells of the cyanobacterium *Synechocystis* PCC 6803. *Photosynth Res* 145:227–235 (IF:3.2).
- Rehman AU, Kodru S, Vass I (2016) Chloramphenicol mediates superoxide production in photosystem II and enhances its photodamage in isolated membrane particles. *Front Plant Sci* 7:1–5. (IF:4.9)
- Kodru S, Sass L, Patil P, et al (2021) Identification of the AG afterglow thermoluminescence band in the cyanobacterium *Synechocystis* PCC 6803. *Physiol Plant* 171:291–300. (IF:4.1)

Other publications:

- Patil PP, Vass I, Kodru S, Szabó M (2020) A multi-parametric screening platform for photosynthetic trait characterization of microalgae and cyanobacteria under inorganic carbon limitation. *PLoS ONE* 15(7): e0236188. (IF:2.7)

International conference abstracts and poster presentations

- Sandeesh Kodru, Ateeq ur Rehman and Imre Vass: How does chloramphenicol affect PSII photoinhibition in isolated spinach thylakoid membranes? (Straub conference at BRC Szeged, Hungary, 3-4 June, 2015).
- Sandeesh Kodru, Ateeq ur Rehman, Milán Szabó and Imre Vass: The role of chloramphenicol in enhancing photodamage and oxygen uptake in isolated PSII, thylakoids and in intact *Synechocystis* (Straub conference at BRC Szeged, Hungary, 24-25 may, 2018)
- Sandeesh Kodru, Ateeq Ur Rehman, Imre Vass: Chloramphenicol enhances Photosystem II photodamage via superoxide Production (14th Nordic Photosynthesis Congress, Turku, Finland 22-24 May 2019)
- Imre Vass, Sandeesh Kodru, Ateeq Ur Rehman: Singlet oxygen production and

photodamage of Photosystem II are enhanced in the absence of Photosystem I in *Synechocystis* PCC 6803 (14th Nordic Photosynthesis Congress, Turku, Finland 22-24 May 2019)

- Sandeesh Kodru, Ateeq Ur Rehman, Imre Vass: Chloramphenicol enhances Photosystem II photodamage via superoxide Production (Straub conference at BRC Szeged, Hungary, 30-31 may, 2019)

Acknowledgements

This dissertation crowns the work conducted in Dr. Imre Vass's lab. I would like to express my special thanks of gratitude to my supervisor **Dr. Imre Vass** for giving me an opportunity to do research, for his patience, motivation, enthusiasm and immense knowledge. His guidance has helped me throughout the research and in the writing of the thesis. It was a great privilege and honor to work and study under his guidance. His support was really influential in shaping my experiment methods and critiquing my results.

I am much obliged to **Dr. Petar H. Lambrev** for his constructive criticism, suggestions to improve my thesis and being a reviewer of the home defense of my thesis.

Apart from my Supervisor, I won't forget to express the gratitude to rest of the team: **Dr. Ateeq Ur Rehman, Dr. Milán Szabó and Dr. Péter Kós** for giving the encouragement and sharing insightful suggestions. They all have played a major role in polishing my research writing skills. Their endless guidance is hard to forget throughout my life.

I would also like to thank **László Sass** for his help in thermoluminescence work and kind support in data analysis.

Thank you to past and present members of the laboratory of molecular stress and photobiology for professional help and the ability to solve almost any problem: **István, Kenny, Gábor, Barbara, Faiza, Ivy, Pritwi, Miklós, Priyanka and Sabit**. I appreciate all the work you have done on my behalf and for a cherished time spent together in the lab, and in social settings.

Thanks to **Györgyi and Lilla** for their technical support. I would also like to thank the administration of the Biological research center for its support, dedication and incredible work on behalf of international students.

Thanks to my friends for all your unwavering support and for reminding me to take breaks and have fun when I have been stressed out.

I am extremely grateful to my **parents** for their love, caring, sacrifices for educating and preparing me for the future. Without their tremendous understanding and encouragement in the past few years, it would be impossible for me to complete my study. Also, I express my thanks to my **sister, brother, sister-in-law and brother-in-law** for their encouragement and support.

- Sandeesh Kodru

Declaration

As the corresponding author, I declare that the author Sandeesha Kodru contributed significantly to the results of the scientific publications listed below. I attest that the results presented in this thesis were not presented in any other PhD thesis.

- i. **Kodru S**, Rehman AU, Vass I (2020) Chloramphenicol enhances Photosystem II photodamage in intact cells of the cyanobacterium *Synechocystis* PCC 6803. *Photosynth Res* 145:227–235.
- ii. Rehman AU, **Kodru S**, Vass I (2016) Chloramphenicol mediates superoxide production in photosystem II and enhances its photodamage in isolated membrane particles. *Front Plant Sci* 7:1–5.
- iii. **Kodru S**, Sass L, Patil P, et al (2021) Identification of the AG afterglow thermoluminescence band in the cyanobacterium *Synechocystis* PCC 6803. *Physiol Plant* 171:291–300.

Szeged, 2021.

Dr. Imre Vass

Scientific adviser, supervisor and corresponding author

